Reconstruction of the 1374 Rhine river flood event around Cologne region using 1D-2D coupled hydraulic modelling approach

Ngo, Hieu; Bomers, Anouk; Augustijn, Denie C.M.; Ranasinghe, Roshanka; Filatova, Tatiana; van der Meulen, Bas; Herget, Jürgen; Hulscher, Suzanne J.M.H.

DOI
10.1016/j.jhydrol.2022.129039

Publication date
2023

Document Version
Final published version

Published in
Journal of Hydrology

Citation (APA)
Ngo, H., Bomers, A., Augustijn, D. C. M., Ranasinghe, R., Filatova, T., van der Meulen, B., Herget, J., & Hulscher, S. J. M. H. (2023). Reconstruction of the 1374 Rhine river flood event around Cologne region using 1D-2D coupled hydraulic modelling approach. *Journal of Hydrology*, *617*, Article 129039. https://doi.org/10.1016/j.jhydrol.2022.129039

Journal of Hydrology 617 (2023) 129039

Contents lists available at ScienceDirect

Journal of Hydrology

journal homepage: www.elsevier.com/locate/jhydrol

Research papers

Reconstruction of the 1374 Rhine river flood event around Cologne region using 1D-2D coupled hydraulic modelling approach

Hieu Ngo [a,b,*], Anouk Bomers [b], Denie.C.M. Augustijn [b], Roshanka Ranasinghe [b,c], Tatiana Filatova [d], Bas van der Meulen [e], Jürgen Herget [f], Suzanne J.M.H. Hulscher [b]

[a] University of Twente, Department of Governance and Technology for Sustainability, Drienerlolaan 5, Enschede 7522 NB, the Netherlands
[b] University of Twente, Water Engineering & Management Department, Drienerlolaan 5, Enschede 7522 NB, the Netherlands
[c] IHE Delft, Coastal & Urban Risk & Resilience Department, Westvest 7, Delft 2611 AX, the Netherlands
[d] Delft University of Technology, Multi Actor Systems Department, Delft 2628 CN, the Netherlands
[e] Utrecht University, Department of Physical Geography, Princetonlaan 8a, Utrecht 3584 CB, the Netherlands
[f] University of Bonn, Department of Geography, Meckenheimer Allee 166, Bonn 53115, Germany

ARTICLE INFO

Keywords:
Rhine river
Historic flood reconstruction
1D-2D coupled hydraulic model
Flood frequency analysis

ABSTRACT

Reconstructions of the most severe historic flood events contribute to improved quantification of design discharges corresponding to large return periods. Reducing the uncertainty of design discharges has a great significance in constructing proper flood defences to protect the hinterland from future flooding. However, reconstructions of the peak discharges of such historic flood events are generally associated with large uncertainties, which arise from the accuracy of the historic topography, hydraulic roughness of the river channels and floodplains, and the historic hydrograph shape. This study sets up a one dimensional-two dimensional (1D-2D) coupled hydraulic model, stretching from the upstream of Bonn at Remagen to downstream of Düsseldorf, Germany, with the length of 113 km to reconstruct the maximum discharge of the 1374 flood event ($Q_{max,1374}$), which is considered to be the largest flood of the last millennium in the Lower Rhine catchment. An uncertainty analysis was performed by adopting different river bed levels and roughness values in order to estimate the influence of these uncertainties on the reconstructed peak discharge. The upstream discharge wave was varied corresponding to a wide range of peak discharges from 12,000 to 24,000 m^3/s. The resulting $Q_{max,1374}$ was determined of between 14,400 and 18,500 m^3/s, were then used in a flood frequency analysis to determine the design discharges corresponding to different return periods. Compared to the design discharge computed with previous estimations of the 1374 peak discharge, we found a significant reduction of 2,000 m^3/s in the design discharge corresponding to a 100,000 year return period, which is the maximum safety standard adopted in the Dutch water policy for some downstream dike sections.

1. Introduction

Floods are one of the main natural hazards causing large damage and human casualties worldwide (Alfieri et al., 2017; Arnell and Gosling, 2016; Hirabayashi et al., 2013). Even though flood risk is expected to increase due to climate and land use change (Alfieri et al., 2015; Brádzil et al., 2006; Hirabayashi et al., 2013), flood events have been a threat since humans began occupying the floodplains of major rivers (Stanley et al., 2001; Wu et al., 2014; Zhang et al., 2005). Nowadays, for many rivers, design discharges corresponding to a specific return period are used to construct flood defences to protect the hinterland from extreme flood events. These design discharges are generally determined by using a flood frequency analysis. In such an analysis, the annual maximum discharges of a measured data set, or peak values that exceed a certain threshold are selected, which are then used to determine the parameters of a probability distribution function (Bezak et al., 2014; Gaume, 2018; Lang et al., 1999; Schendel and Thongwichian, 2017). From this fitted distribution function, discharges corresponding to different return periods are derived.

In many countries (e.g. the Netherlands, Norway, Germany, UK, US), the discharges corresponding to large return periods (e.g. 1000 years, 10,000 years, 100,000 years) are used to design important flood

* Corresponding author.
E-mail address: h.q.ngo@utwente.nl (H. Ngo).

https://doi.org/10.1016/j.jhydrol.2022.129039
Received 30 August 2022; Received in revised form 22 December 2022; Accepted 24 December 2022
Available online 29 December 2022

defences (e.g. dams, flood barriers, dikes). However, the length of measured discharge data is usually insufficient for a robust flood frequency analysis (Cameron et al., 1999; Engeland et al., 2018; Gebregiorgis and Hossain, 2012; Van Alphen, 2016, Vorogushyn et al., 2012). Using the limited measured discharge data set to extrapolate to a design discharge corresponding to such large return periods results in large uncertainty intervals. In addition to the lower bound of the uncertainty interval that is crucial for flood protection policymaking, the upper bound is also important since an extreme overestimation of the design discharge caused by extrapolation may result in unnecessarily large investments. To reduce these uncertainty intervals, the data set of measured discharges can be extended with reconstructed historic flood events (e.g. Bomers et al., 2019a; Frances et al., 1994; MacDonald et al., 2014; Sartor et al., 2010). In other words, improved quantification of design discharges corresponding to large return periods can be achieved by precise reconstruction of the most severe historic flood events. Therefore, many studies have focused on reconstructing historic flood discharges based on various sources such as written records, flood marks, and flood deposits (Balasch et al., 2010; Benito et al., 2021; Bomers et al., 2019b; Bomers et al., 2019c; Elleder et al., 2013; Herget and Meurs, 2010; O'Connell et al., 2002; Payrastre et al., 2011; Reis and Stedinger, 2005; Ruiz-Bellet et al., 2014; Stamataki and Kjeldsen, 2021; Toonen et al., 2013; Toonen et al., 2015; Van der Meulen et al., 2021).

Discharge magnitudes of historic flood events can be reconstructed by using the cross-sectional approach or longitudinal approach (these two approaches are collectively referred to as simple approaches) (Herget and Meurs, 2010; Webb and Jarrett, 2002) or multidimensional hydraulic modelling approach (2D and 3D hydraulic models) (Lang et al., 2003; Sheffer et al., 2003; Van der Meulen et al., 2021, Van Doornik, 2013). However, reconstructed peak discharges of historic flood events are generally associated with large uncertainties arising from inaccuracies in the historic topography, hydraulic roughness of the main river and floodplains, and historic hydrograph shape (Benito and Thorndycraft, 2003; Herget and Meurs, 2010; Lang et al., 2003; Lang et al., 2004). Simple approaches can only account for uncertainties in spatial components at selected cross-section locations but not in the river system as a whole. In addition, these approaches can also only consider the effect of peak discharge on river water levels, without the hydrograph shape. While hydrograph shapes affect water levels and flooding parameters (e.g. flood extent, inundation depth, duration) (Bomers et al., 2019d; Dung et al., 2015; Pol, 2014). In contrast, using a multidimensional hydraulic modelling approach allows for taking into account spatial uncertainties and discharge waves (peak discharge and flood hydrograph shape) on river water levels (Bomers et al., 2019b; Lang et al., 2003; Lang et al., 2004). Hence, this approach can simulate spatial components and river flow closer to reality than simple approaches.

Many hydraulic models such as MIKE, Delft3D, HEC-RAS, ISIS (now Flood Modeller), SOBEK, LISFLOOD-FP have been developed over the last decades to address the complex real-world hydraulic problems (Bomers et al., 2019b; Horritt and Bates, 2002; Pasquier et al., 2018; Van et al., 2012). These hydraulic models calculate a rating curve *Q(h)* by solving the Saint-Venant equations (also referred to as the shallow water equations), representing the flow in natural rivers and floodplains. 1D hydraulic models are commonly used to provide estimates of the flow depth and velocity at locations in the river system with a low computational cost. However, they are unsuitable for accurately simulating flood propagation, especially the complex 2D flow in floodplains. In contrast, 2D depth-averaged hydraulic models can better simulate complex flow patterns and provide more accurate results. The main disadvantages of 2D hydraulic models are that they require more in-depth data regarding topography and resistance data, and have a large computational cost. Therefore, using 2D hydraulic models is generally not deemed suitable for reconstructions of historic flood events, especially when uncertainty analysis regarding the most uncertain parameters of the river and floodplains (river bathymetry, floodplain topography, hydraulic roughness) are also required, necessitating several different simulations. In recent years, the coupling between 1D and 2D hydraulic models has become popular to combine advantages of both approaches (Adeogun et al., 2015; Bomers et al., 2019b; Cardoso et al., 2020; Dasallas et al., 2019; Fan et al., 2017; Leandro and Martins, 2016; Pasquier et al., 2019, Van der Meulen et al., 2021). The coupling of 1D and 2D hydraulic models enhances computational efficiency compared to 2D hydraulic models while improving the accuracy of model results compared to 1D hydraulic models (Dasallas et al., 2019; Fan et al., 2017; Leandro et al., 2016). In this study, we use a 1D-2D coupled hydraulic modelling approach to reconstruct the $Q_{max,1374}$ in the Rhine river at Cologne, in which the river is modelled by 1D profiles and the floodplains are discretized on a 2D grid.

In this paper, Section 2 presents the case study, followed by the method adopted for reconstructing the 1374 historic flood event in Section 3. Next, Section 4 describes modelling results and presents discussion on (1, 2) the effect of flood hydrographs and the land cover classes distribution on the water levels; (3) the effect of the discharge of the Sieg and Wupper tributaries on water levels; (4) the difference in $Q_{max,1374}$ between previous studies and this study; and (5) the magnitude of design discharges. Finally, the paper ends with conclusions in Section 5.

2. Case study

The Rhine river is one of the major rivers in Europe, with a length of 1,230 km and an average discharge of about 2,200 m^3/s at Lobith in the Lower Rhine (Te Linde et al, 2011). It originates from the Alps in Switzerland and flows through Germany and the Netherlands, and debouches into the North Sea (Fig. 1a). In this study, we consider an area of 991 km^2 of the Rhine river catchment, stretching from upstream of Bonn to downstream of Düsseldorf, Germany with the length of 113 km (Fig. 1b). The upstream boundary of the study area is placed 15 km upstream of the city of Bonn at Remagen, just upstream where the Rhine river enters the alluvial reaches of the Lower Rhine valley (Erkens et al., 2011; Klostermann, 1992; Van der Meulen et al., 2020). In addition, the distance from the upper boundary at Remagen to Cologne and Urdenbach are 32.5 and 81 km, respectively.

2.1. The 1374 flood event and related historic flood marks

The first months of 1374 were characterized by a continuous flood event in several catchments throughout Central Europe (numerous source texts are compiled in Alexandre, 1987; Buismann, 1996; Weikinn, 1958). Evidence is handed down mainly by written reports from northern France including Paris, Belgium, The Netherlands and towards Bremen in northern Germany for the northward margin of occurrence. The River Weser and Vlatava valleys including Prague mark the eastern limits and Strasbourg in Alsace towards Ulm at Danube River the southern one. Due to the long time and missing motivation of quantitative monitoring, water level reports of the flood event are rather rare. As a characteristic of Central Europe, precipitation occurred by snow and rain with cold periods, which resulted in increased discharges due to additional meltwater supply to intensive, long lasting rainfall (Krahe, 1997).

Generally speaking, discharge of the northern parts of the Rhine river was characterized by high water levels lasting from late December 1373 until April 1374. At Cologne, peak levels are reported from January 4th, January 25th and February 9-11th, 1374. The pattern of three peaks is confirmed for the Lower Rhine (Fig. 1a) section with minor delays for January 6th and 21st-25th and February 9-15th. The flood event in February is assumed to have the highest water level ever observed at Cologne in the past (Krahe, 1997), besides the ice-jam flood in 1784 (Brázdil et al., 2010). Based on the report of boats crossing the city fortification, the minimum water level during peak discharge at Cologne can be estimated as 47.70 m above sea level (asl). The maximum flood

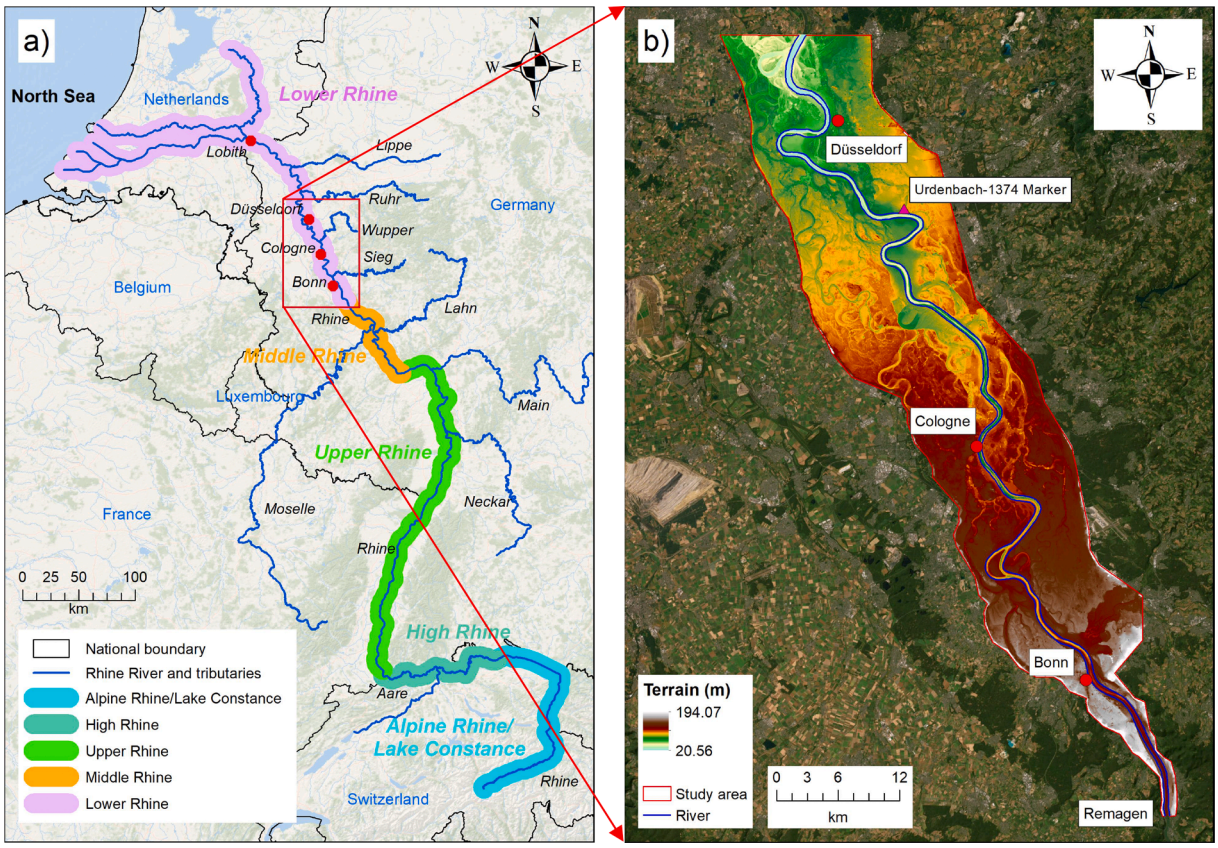

Fig. 1. (a) Rhine river catchment, (b) The study area stretches from upstream of Bonn at Remagen to downstream of Düsseldorf with a DEM data for the study area (Source: Van der Meulen et al. 2021a). The course of the Rhine river in Fig. 1b is given as it was before the 1374 flood event.

water level is estimated to be 48.50 m asl based on the report of the steps of St. Georgius monastery not being reached (Herget and Meurs, 2010). With the above arguments, the authors suggest a representative value of 48.28 m asl for the flood peak level at Cologne. Note that all elevation levels mentioned above were transferred to the modern period reference level of the current gauge at an elevation of 34.98 m asl at Cologne.

The second location with water level information of the flood event from within the area of investigation is a flood level marker given at a house in Urdenbach (Fig. 2), located just upstream of the city of Düsseldorf. Geodetic surveys result in an elevation of 41.69 m asl. The marker is installed at a house located in the valley of Itter Creek, a minor local tributary of the River Rhine, approximately 500 m upstream of the ancient confluence. Due to the gentle slope and short distance, the water level of the creek is assumed equal to the Rhine river during flood events as documented by the repeated flood marks on the building. According to the owner of the house, the inscription was found during renovation of the house and modified by appearance for better visibility. The validity of the marker could not be verified so far, but it should be noted that the house itself was built in approximately 1709, several centuries after the flood event. Unfortunately, it is not known so far who made the first inscription of the flood level and what information the elevation is based on. It might be speculated that during the inscription of the water level of the ice-jam flood of January 1784, the previous top record of water level in 1374 was re-marked.

Fig. 2. Water level related to the 1374 flood event at Düsseldorf-Urdenbach (Photo: Jürgen Herget).

3. Methodology

To reconstruct the $Q_{max,1374}$, we used an "inverse modelling" approach (Van der Meulen et al., 2021). First, the 1D-2D coupled hydraulic model was set up with the past terrain (river bathymetry and floodplains topography), and hydraulic roughness coefficients for land cover classes corresponding to the medieval situation to simulate discharge waves with different peak discharges. An uncertainty analysis was then performed to investigate the effects of the uncertain input parameters (river bathymetry and floodplains topography, and hydraulic roughness coefficients) on the $Q_{max,1374}$. Subsequently, the simulated water levels were compared with the flood marks (observed water levels) corresponding to the 1374 flood event at Cologne and Düsseldorf-Urdenbach to determine the appropriate discharge magnitude at the upstream boundary.

The estimated $Q_{max,1374}$ was used to extend the historical discharge data set. A flood frequency analysis was then performed based on the extended discharge data set to determine the design discharges and their

95 % confidence interval for different return periods.

3.1. Data

3.1.1. Topography and bathymetry

The past river bathymetry and floodplain topography play an important role in reconstructing historic flood events (e.g. Benito and Thorndycraft, 2004; Herget and Meurs, 2010; Lang et al., 2004). However, these data for the year 1374 are not available. Therefore, a section of the palaeo-DEM with a 10 m resolution of the Lower Rhine valley and upper delta in early medieval times (circa 800 CE) (Fig. 1), reconstructed by Van der Meulen et al. (2020), was used for this study. This palaeo-DEM was reconstructed based on a ground-level LiDAR DEM, which was obtained by merging the available LiDAR data (AHN2 in the Netherlands National Grid and DGM1 resampled from the German to the Netherlands Grid) and inserting the river bathymetry from the RWS-LANUV Baseline datasets. The LiDAR DEM was corrected for elevation change due to the recent mining-induced subsidence (Harnischmacher and Zepp, 2014). Existing geological mapping datasets were then used to demarcate inactive and active zones in the DEM (see Van der Meulen et al., 2020 for more details). All anthropogenic relief elements were removed using separate procedures for linear (e.g. roads, railroads, dikes) and non-linear (e.g. pits, raised grounds for buildings, dump sites) elements to obtain the palaeotopography of the inactive zone. Then, geological and historical geographical information were incorporated to reconstruct the natural floodplain topography and the river position and bathymetry in the active zone for the target age of palaeo-DEM (Van der Meulen et al., 2020).

In this study, it was assumed that there were no significant interventions in the floodplains between the 800 CE and 1374. Furthermore, due to wide floodplains, a few centimeters of sediment accumulation (Herget and Meurs, 2010) do not make much difference in the floodplain elevation between the 800 CE and 1374. These assumptions justify the use of the 800 CE floodplain topography in our study. However, different from floodplains, the river bed varies considerably over time scales of centuries due to erosion and deposition, although this process is stronger in downstream river reaches (Van der Meulen et al., 2020).

There is a significant difference in the Rhine river bathymetry at Cologne between the selected palaeo-DEM and a cross-sectional reconstruction by Herget and Meurs (2010). Herget and Meurs (2010) reconstructed the discharge magnitude of historic flood events in the Rhine river at Cologne, including the 1374 flood event by using a relatively simple cross-sectional approach. They defined the river cross-section at Cologne corresponding to the year 1374 based on the river bathymetry at Cologne surveyed in 1895 (Jasmund, 1901) and a river incision rate of 0.1 cm per year. The river-cross section in 1374 was determined by raising the river-cross section in 1895 by a value corresponding to the product of the incision rate and the time length (years) between the two years 1895 and 1374. According to Herget and Meurs (2010), the lowest elevation in the cross-section at Cologne corresponding to the year 1374 was approximately 33 m asl (red circle in Fig. 3a). In comparison, the lowest elevation in the cross-section at Cologne extracted from the palaeo-DEM used in this study is 36.2 m asl (blue circle in Fig. 3a), representing a difference of 3.2 m. Human activities such as dredging to improve navigation were only carried out later than 1895 (Herget and Meurs, 2010). Therefore, the difference in the river bathymetry can be explained by (1) the accuracy of the palaeo-DEM, (2) the incision rate used in the study of Herget and Meurs (2010) is smaller compared to the reality, (3) the effect of large flood events in the period from 800 CE to 1895 (e.g. 1342, 1374, 1497, 1595 flood events), which could cause significant erosion to the riverbanks and beds (Baynes et al., 2015; ENW Hoogwater, 2021; Matsumoto et al., 2016), and (4) combinations of reasons 1, 2 and 3. With this significant

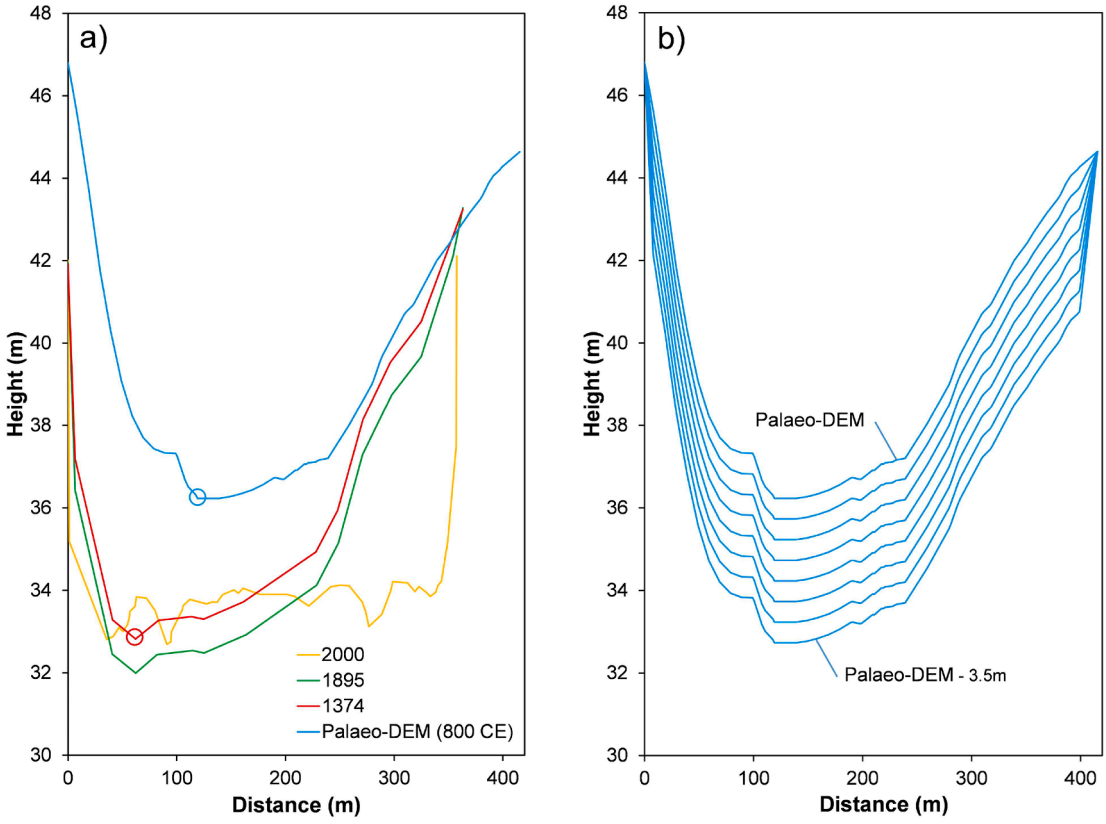

Fig. 3. (a) Comparison of cross-section at Cologne extracted from palaeo-DEM of Van der Meulen et al. (2020) for ~ 800 CE with cross-section data for the years 2000, 1895 and 1374 in Herget and Meurs (2010) at Cologne, (b) different river bed levels used in the uncertainty analysis.

difference, river bathymetry is included in an uncertainty analysis to investigate its effect on the $Q_{max,1374}$ by lowering all 1D cross-sections representing the main river extracted from palaeo-DEM with reduced intervals of 0.5 m in level up to 3.5 m (Fig. 3b).

3.1.2. Hydraulic roughness

The hydraulic roughness is expressed as Manning's *n* values, which represent the resistance to flow in river channels and floodplains. This is an important parameter that greatly affects the water level for a given discharge. Van der Meulen et al. (2021) divided the medieval Lower Rhine valley and delta into five different landscape classes based on the distance to the river and relative floodplain elevation, with distinctive land cover (natural vegetation and land use) characteristics, and distinctive hydraulic roughness values (Fig. 4). Here, the average roughness coefficient for each landscape classes (n_{best}) (Table 1; see Van der Meulen et al. (2021) for details) is applied in all simulations. In addition, the lower (n_{min}) and upper estimates (n_{max}) of Manning's n values (Table 1) were included in the uncertainty analysis to account for uncertainties in the $Q_{max,1374}$ that are associated with the hydraulic roughness parameter.

3.2. Hydraulic model set-up

A 1D-2D coupled hydraulic model in HEC-RAS (Brunner, 2016) was set up for the study area. The main channel of the Rhine river was schematized by 500-m-spaced 1D profiles along the river channel, while the floodplains were discretized on a 2D grid with a resolution of 200×200 m (Fig. 5). The 1D profiles are connected to the 2D grid cells

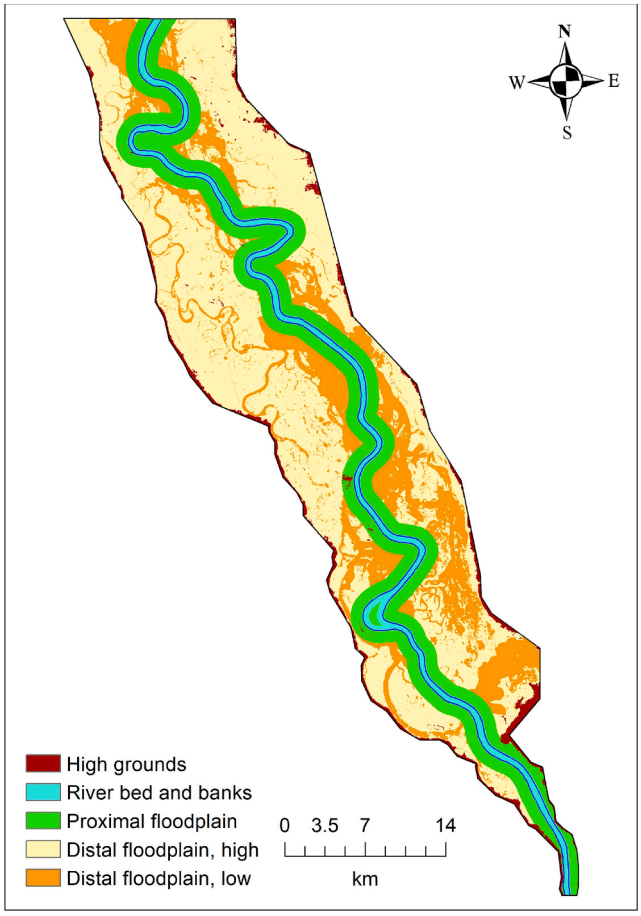

Fig. 4. Distribution of roughness classes in the study area. The abbreviations and Manning's *n* values attributed to the different classes are given in Table 1 (Source: Van der Meulen et al. (2021a)).

Table 1
Overview of parameters that were varied for uncertainty analysis.

Q_{peak} (m^3/s)	Manning's n values for landscape classes				River bed level (m)
	Class	n_{min} ($s/m^{1/3}$)	n_{best} ($s/m^{1/3}$)	n_{max} ($s/m^{1/3}$)	
12,000	High grounds	0.100	0.100	0.100	palaeo-DEM
14,000					palaeo-DEM − 0.50 *m*
	River bed and banks	0.025	0.030	0.045	
16,000		0.060	0.070	0.080	palaeo-DEM − 1.00 *m*
	Proximal floodplain	0.040	0.050	0.060	
18,000		0.035	0.040	0.055	palaeo-DEM − 1.50 *m*
	Distal floodplain, high				
20,000					palaeo-DEM − 2.00 *m*
	Distal floodplain, low				
22,000					palaeo-DEM − 2.50 *m*
24,000					palaeo-DEM − 3.00 *m*
					palaeo-DEM − 3.50 *m*

using the weir equation. Since the flow regime in the natural river and its floodplain are unsteady and highly complex, the full momentum equations are used to solve the system (Brunner, 2016).

Hydraulic structures along the river (e.g. bridges, weirs, embankments) influence the river water levels (Brunner, 2016; Costabile et al., 2015; Teraguchi et al., 2011). The present study focuses on the historic flood event in 1374 (almost 650 years ago) with limited information about the recorded water levels (flood marks) and the structures (e.g. bridges, weirs) in the study area. Maps of Cologne and its surrounding for 1571 (by Mercator) and 1792 (by Wiebeking) (Figs. 6 and 7) showed that there was no appearance of special structures (bridges or weirs). While Cologne is a large city located next to the Rhine river with many historical activities in Roman times. Therefore, it is likely that also no special structures were present in the Düsseldorf-Urdenbach area, which is located between the two large cities of Cologne and Düsseldorf. Furthermore, the water level during the 1374 flood event was extremely high, and boats could cross the city's walls in Cologne. It means the maximum water level was much higher than the bridges and weirs (if present). Therefore, we assume that we can neglect the influence of hydraulic structures on the water levels along the river during the 1374 flood event. Consequently, these hydraulic structures are not simulated in the model for the study area.

3.2.1. Boundary conditions

Discharge waves at Remagen were used as the upstream boundary condition of the model (Fig. 5). An initial discharge of 1000 m^3/s was used in all runs to avoid a dry channel at the beginning of the simulations. A normal depth was implemented as the downstream boundary condition of the model, which was computed based on the friction slope, the flow, Manning's *n* value and the specified cross-section shape using Manning's equation (Brunner, 2016).

There are two main tributaries of the Rhine river located in the model domain, namely the Sieg river and Wupper river (Fig. 1a). Therefore, the flows of the Sieg and Wupper tributaries were included in the model as lateral inflows (Fig. 5). However, the historic discharge magnitude at the Sieg and Wupper tributaries in 1374 is uncertain. In this study, the discharge time series in 1926 of the Sieg tributary and the discharge time series in 1957 of the Wupper tributary (Fig. 8a) corresponding to the largest measured discharges so far, were used to represent the lateral inflow at the Sieg and Wupper in all simulations. The flood peak of these events occurred at different times. However, in this study the flood peak of these events was shifted to the same time that the flood peak occurred at Remagen to investigate the resonance of these flood events to downstream water levels at points of interest (Cologne and Düsseldorf-Urdenbach).

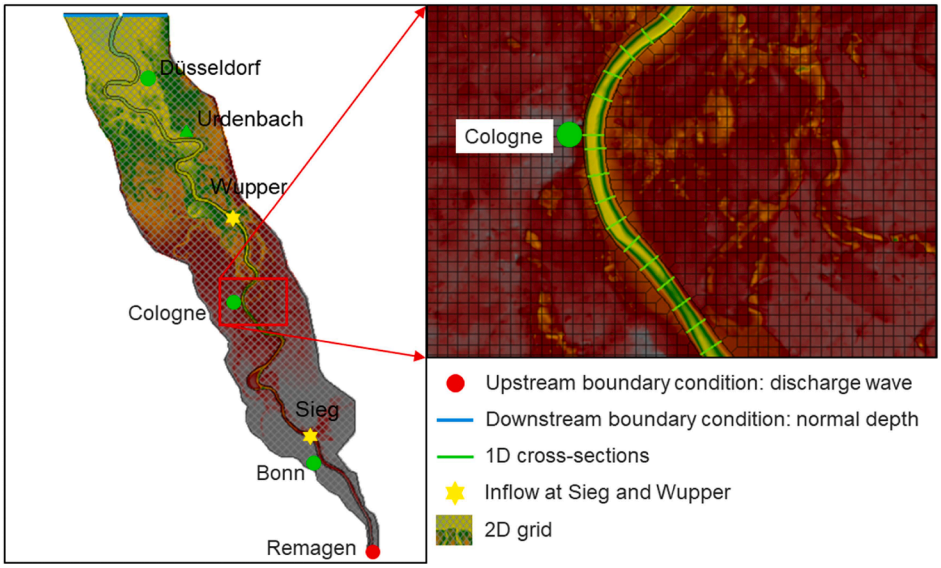

Fig. 5. The model set-up for the study area (left side) and the close-up of the 2D grid (right side).

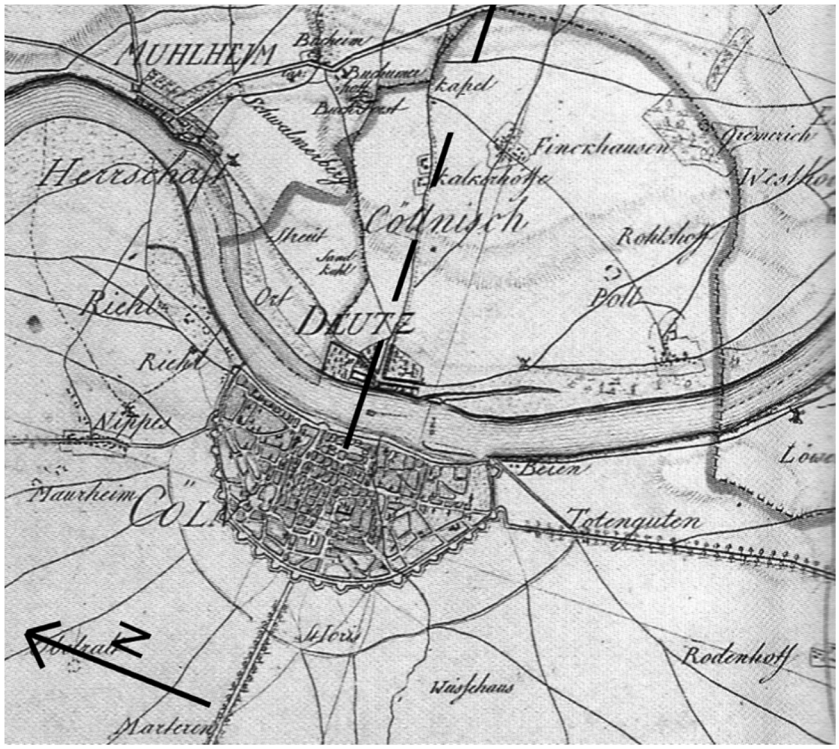

Fig. 6. Map of Cologne and its vicinity by Wiebeking in 1792 ().
Source: Herget and Meurs, 2010

3.2.2. *Model calibration*

Model calibration cannot be performed for a case that lacks data. In this case, we only have the two flood marks corresponding to the 1374 flood event available at Cologne and Düsseldorf-Urdenbach. In addition, the accuracy of the topography of the river channel and its floodplains, and historic landscape classes is highly uncertain, as is inherently the case for any terrain reconstruction with a target age prior to the onset of accurate land surveying techniques and records. Nevertheless, a reasonable reconstruction of the $Q_{max,1374}$ with the model is feasible via performing an uncertainty analysis in which uncertain parameters are systematically varied (river bathymetry, hydraulic roughness) together with a range of discharge waves.

Discharge waves (peak discharge and flood hydrograph shape) at the upstream affect downstream water levels (Bomers et al., 2019d; Dung et al., 2015; Pol, 2014). However, for historic flood events, both the peak discharge value and hydrograph shape are commonly uncertain. Therefore, in this study, the flood hydrograph shape of the 1926 flood event (Fig. 8b), see e.g. Bomers et al (2019c), which is the largest historical measured discharge in the Rhine river at Andernach so far, was selected to represent a standard hydrograph shape to reconstruct the $Q_{max,1374}$.

The $Q_{max,1374}$ values are discussed in detail by, among others, Herget

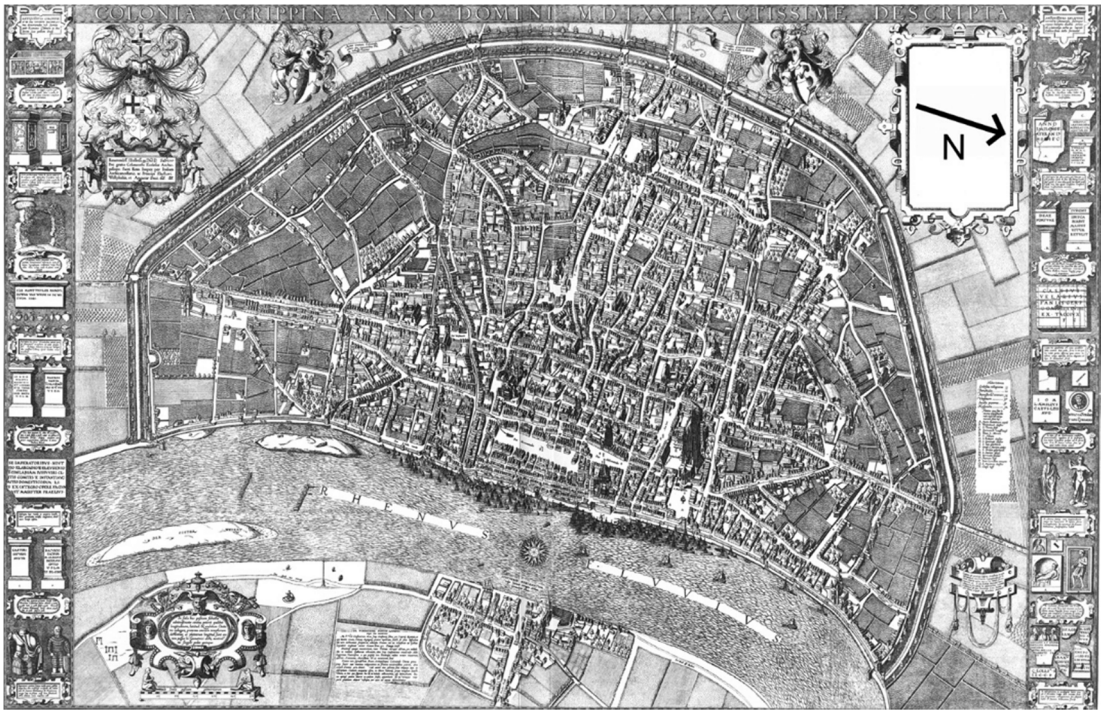

Fig. 7. Map of Cologne by Mercator from 1571 ().
Source: Hansen, 1899

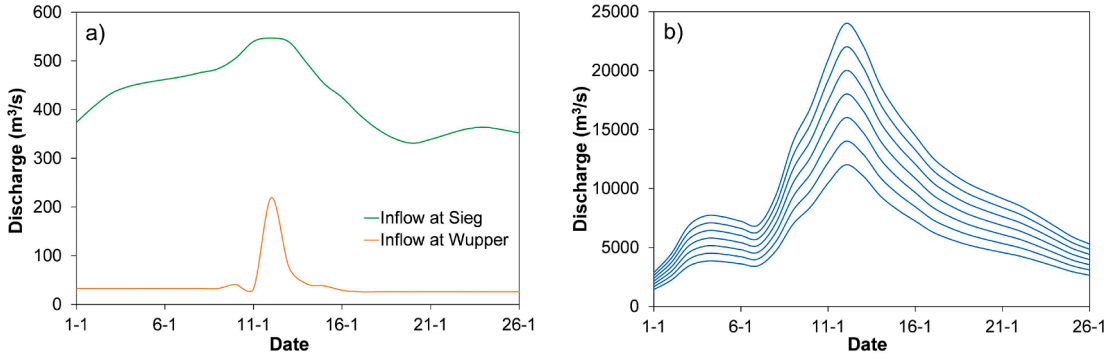

Fig. 8. (a) Flows of the Sieg and Wupper tributaries were used to represent lateral inflows at the Sieg and Wupper in all simulations, (b) seven discharge waves were used as the upstream boundary condition near Remagen, Germany.

and Meurs (2010), Toonen (2013), Van Doornik (2013), Hegnauer et al. (2014), Hegnauer et al. (2015), Van der Meulen et al. (2021), Van der Meulen (2021) and Van der Meulen et al. (2022). Herget and Meurs (2010) found a peak discharge range of the 1374 flood event ranging between 18,800 m^3/s and 29,000 m^3/s. Van Doornik estimated the $Q_{max,1374}$ between 18,500 m^3/s and 21,200 m^3/s. However, as argued by Van der Meulen (2021), the $Q_{max,1374}$ is most likely between the largest measured discharge of ~12,000 m^3/s and the largest discharges of ~24,000 m^3/s generated by stochastic weather simulations coupled to hydrological models (Hegnauer et al., 2014; Hegnauer et al., 2015). Therefore, in this study, the upstream boundary conditions were created by re-scaling the discharge wave of the 1926 flood event to peak discharge values varying from 12,000 to 24,000 m^3/s with intervals of 2000 m^3/s (Fig. 8b).

3.3. Uncertainty analysis

A total of 168 simulations were performed in the uncertainty analysis, which are the combinations of different discharge waves (7 peak discharge values) with different Manning's n values (n_{best}, n_{min} and n_{max}) and the different river bed levels (8 values) (Table 1) to determine the $Q_{max,1374}$.

In addition to performing the above simulations for uncertainty analysis, we also conducted additional simulations to evaluate the effect of flood hydrograph shapes and the distribution of land cover classes on the $Q_{max,1374}$ as outlined below:

- Flood hydrograph shapes

As mentioned in Section 2, the year 1374 witnessed one large flood events with three peaks in the early months with high water levels at Cologne around January 4th, January 25th, and around February 9th to 11th (see references in Herget and Meurs, 2010; Van der Meulen, 2021). Therefore, besides the flood hydrograph shape of the 1926 flood event with one peak (red curve in Fig. 9), used to reconstruct the $Q_{max,1374}$, we selected two other flood hydrograph shapes with 3 peaks (Fig. 9) to investigate the effect of their shapes on the water level at Cologne and Düsseldorf-Urdenbach. From the dataset of all the GRADE-simulated

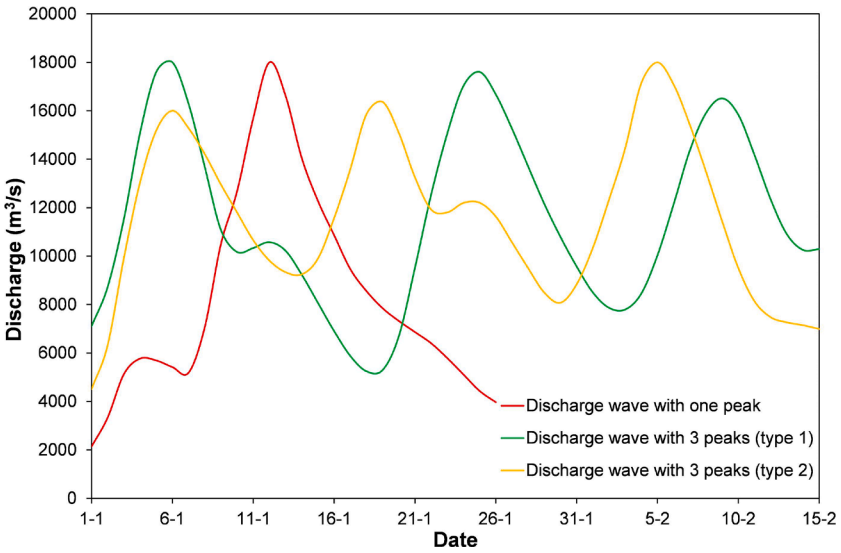

Fig. 9. Three different extreme hydrograph shapes were scaled with their highest flood peaks to 18,000 m^3/s.

(GRADE – Generator of Rainfall and Discharge Extremes (Hegnauer et al., 2014)) discharge waves (50,000 years), we extracted all years having flood hydrograph shapes with three peaks exceeding a discharge volume of 10,000 m^3/s spaced within a period of 10–25 days. In the obtained hydrograph shapes, we selected two hydrograph shapes that match the description of the 1374 flood event. These include (1) a flood hydrograph shape with three peaks with the first peak having the maximum discharge (type 1 in Fig. 9) and (2) a flood hydrograph shape with three peaks with the third peak having the maximum discharge (type 2 in Fig. 9). These flood hydrograph shapes are expected to represent realistic hydrograph shapes that may occur under current climate conditions (Hegnauer et al., 2014). These two flood hydrograph shapes were scaled such that the maximum peak value corresponds with a discharge magnitude of 18,000 m^3/s (Fig. 9), which might approximate the $Q_{max,1374}$ (Van der Meulen et al., 2022).

- The distribution of landscape classes

Besides Manning's *n* values of the landscape classes, the spatial distribution of the landscape classes also affects river water levels. The distribution of the Proximal floodplain (P) class in the land cover map (Fig. 3) used in this study is constant along the river, with a width of 1,000 m on both sides of the river (Van der Meulen et al., 2021), which may not be the case in reality. Therefore, we investigated the effect of the distribution of this landscape class on the $Q_{max,1374}$ by merging this class with the low distal floodplain (DL) class and using the average roughness coefficient (n_{best}) for these land cover classes. Here, we considered two cases: (1) the Manning's *n* value of P zone is assigned the same value with the Manning's n value of DL zone ($n_P = n_{DL} = 0.04$ s $m^{-1/3}$) (case 1); and (2) the Manning's *n* value of DL zone is assigned the same value of Manning's value of P zone ($n_{DL} = n_P = 0.07$ s $m^{-1/3}$) (case 2).

3.4. The magnitude of design discharges

The data set of measured discharges can be extended with reconstructed historic flood events to get improved quantification of design discharges. This especially applies to design discharges corresponding to large return periods. To test the effect of the $Q_{max,1374}$ on design discharge estimates, the systematic data set covering the period 1772–2018 was extended with 12 reconstructed historic flood events that occurred in the period 1300–1772. These data were used to create a continuous discharge data set covering the period 1317–2018 using a bootstrap method, following the approach of Bomers et al. (2019a). A flood frequency analysis was performed, both considering the $Q_{max,1374}$ by Herget and Meurs (2010) and using the hydraulic modelling approach adopted in this study, to determine the design discharges and their 95 % confidence interval for different return periods based on the generalized extreme value (GEV) distribution function given as:

$$F(x) = \exp\left\{ -\left[\xi \frac{x-\mu}{\sigma}\right]^{\frac{1}{\xi}} \right\} \quad (1)$$

where three parameters, μ, σ, ξ represent a location, scale, shape of the distribution function.

4. Results and discussion

4.1. $Q_{max,1374}$

The maximum simulated water levels and highest flow depths at Cologne and the maximum simulated water levels at Düsseldorf-Urdenbach corresponding to all combinations of uncertain parameters investigated are shown in Tables 2-4. Based on comparisons with flood mark heights at Cologne (48.28 m asl) and Düsseldorf-Urdenbach (41.69 m asl), and flow depth at Cologne (≥13.3 m), there is no value of the $Q_{max,1374}$ corresponding to the uncertainty range of Manning's *n* values and river bed levels resulting in simulated water levels that exactly match both historic flood mark levels at Cologne and Düsseldorf-Urdenbach. This could, however, be due to the lack of accuracy of recorded historic flood marks at Cologne and Düsseldorf-Urdenbach. As mentioned in Section 2, even though the flood mark at Cologne was recorded and described in various reliable sources, it also has a validated uncertainty, while the flood mark at Düsseldorf-Urdenbach was collected recently with unvalidated accuracy. Considering this, here we conclude the $Q_{max,1374}$ at the upstream boundary to be between 14,400 m^3/s and 18,500 m^3/s corresponding to Manning's *n* values and river bed levels below the early medieval level extracted from the palaeo-DEM from 1.5 m to 3.5 m. As shown in Fig. 10, a discharge magnitude of around 18,000 m^3/s may be the most realistic magnitude of the 1374 millennium flood event, as this magnitude combines with the Manning's *n* values (n_{min}, n_{best}, n_{max}) for all land cover classes and river bed levels from 2,5m to 3,5 m below the early medieval level extracted from the palaeo-DEM resulted in simulated water levels closest to historic flood marks at Cologne and Düsseldorf-Urdenbach.

Table 2
The maximum water level at Cologne corresponding to the different combinations of river bed levels with Manning's n values and peak discharges – historic reconstructed maximum water level is 48.28 m asl for Feb. 1374.

River bed level (m)	Manning roughness coefficient	Water level at Cologne (m)						
		12,000 (m^3/s)	14,000 (m^3/s)	16,000 (m^3/s)	18,000 (m^3/s)	20,000 (m^3/s)	22,000 (m^3/s)	24,000 (m^3/s)
palaeo-DEM	n_{max}	49.12	49.49	49.81	50.10	50.37	50.60	50.82
	n_{best}	48.37	48.74	49.06	49.36	49.62	49.86	50.09
	n_{min}	48.00	48.37	48.71	49.00	49.26	49.50	49.72
palaeo-DEM − 0.50 *m*	n_{max}	48.99	49.37	49.71	50.01	50.28	50.52	50.74
	n_{best}	48.19	48.58	48.91	49.21	49.50	49.75	49.98
	n_{min}	47.77	48.19	48.53	48.84	49.12	49.36	49.60
palaeo-DEM – 1.00 *m*	n_{max}	48.85	49.25	49.60	49.91	50.19	50.44	50.66
	n_{best}	47.98	48.40	48.75	49.07	49.36	49.63	49.87
	n_{min}	47.52	47.97	48.35	48.68	48.97	49.22	49.47
palaeo-DEM − 1.50 *m*	n_{max}	48.72	49.12	49.48	49.80	50.09	50.35	50.59
	n_{best}	47.75	48.21	48.58	48.92	49.21	49.50	49.75
	n_{min}	47.24	47.74	48.15	48.50	48.80	49.08	49.33
palaeo-DEM – 2.00 *m*	n_{max}	48.56	48.98	49.35	49.69	49.99	50.26	50.50
	n_{best}	47.50	47.99	48.40	48.75	49.06	49.35	49.62
	n_{min}	46.91	47.47	47.92	48.30	48.62	48.91	49.18
palaeo-DEM − 2.50 *m*	n_{max}	48.40	48.83	49.22	49.57	49.88	50.15	50.41
	n_{best}	47.21	47.76	48.20	48.57	48.90	49.19	49.48
	n_{min}	46.54	47.16	47.67	48.08	48.44	48.74	49.02
palaeo-DEM – 3.00 *m*	n_{max}	48.22	48.69	49.08	49.44	49.77	50.06	50.31
	n_{best}	46.90	47.51	47.99	48.39	48.73	49.05	49.33
	n_{min}	46.12	46.82	47.38	47.84	48.22	48.56	48.84
palaeo-DEM − 3.50 *m*	n_{max}	48.03	48.53	48.94	49.31	49.65	49.95	50.22
	n_{best}	46.54	47.21	47.75	48.18	48.55	48.87	49.16
	n_{min}	45.69	46.44	47.06	47.57	47.98	48.35	48.65

4.2. The effect of the different flood hydrograph shapes on water levels

Figs. 11 and 12 show the water level time series at Cologne and Düsseldorf-Urdenbach corresponding to the combinations of the three flood hydrograph shapes with Manning's n values (n_{best}) and river bed level 3 m below the early medieval level extracted from the palaeo-DEM (which is the elevation of the river cross-section at Cologne that most closely resembles the elevation of the river cross-section used by Herget and Meurs (2010)). The results show hardly any significant differences (up to 4 cm) (Figs. 11 and 12) for the highest water level at Cologne and Düsseldorf-Urdenbach corresponding to these flood hydrograph shapes. In addition, flood extents corresponding to the highest water level in the study area do not differ significantly for the different flood hydrograph shapes (Fig. 13) (391 km^2, 394 km^2 and 396 km^2 corresponding to flood hydrograph shapes with one peak, three peaks type 1 and 2, respectively). These minor difference is explained by (1) the relatively long (12–19 days) time intervals between the flood peaks, (2) the absence of embankments and other flood protection works in the medieval landscape situation of the upper Lower Rhine river, and (3) wide floodplains of the Rhine river in the scope of the study area. The flood hydrograph shape may have a larger effect on maximum water levels and flood extents in river stretches with narrower floodplains, such as the Middle Rhine river upstream of our study area.

4.3. The effect of the distribution of land cover classes on water levels

The results (Figs. 14 and 15) show that the considered change in the spatial distribution of the P land cover class does not significantly affect the maximum water level at Cologne and Düsseldorf-Urdenbach. Specifically, corresponding to the estimated discharge magnitude (14,400–18,500 m^3/s) for the 1374 flood event in section 4.1, the difference in the maximum water level varies from −0.04 m to −0.12 m at Cologne (Fig. 14) and −0.04 m to −0.08 m at Düsseldorf-Urdenbach (Fig. 15) between case 1 (yellow curve) and baseline (red curve) that corresponds to the distribution of P class as reconstructed in Van der Meulen et al. (2021). In comparison, the difference in the water level between case 2 (blue curve) and baseline varies from 0.08 m to 0.13 m at Cologne (Fig. 14) and 0.07 m to 0.11 m at Düsseldorf-Urdenbach (Fig. 15).

4.4. The effect of the discharge of the Sieg and Wupper tributaries on water levels

Table 5 shows the maximum water levels at Cologne and Düsseldorf-Urdenbach corresponding to the simulations that include and exclude the flows of the Sieg and Wupper tributaries for combinations of Manning's n values (n_{best}) and river bed level 3 m below the early medieval level extracted from the palaeo-DEM. The results show that the discharges of the Sieg and Wupper tributaries do not significantly affect the

Table 3
The highest flow depth at Cologne corresponding to the maximum water level – historic reconstruction reveals a flow depth higher than 13.3 m for Feb. 1374 (note that: the highest flow depth is the difference between the highest water level and the lowest point of the river cross-section).

River bed level (m)	Manning Roughness coefficient	Flow depth at Cologne (m)						
		12,000 (m^3/s)	14,000 (m^3/s)	16,000 (m^3/s)	18,000 (m^3/s)	20,000 (m^3/s)	22,000 (m^3/s)	24,000 (m^3/s)
palaeo-DEM	n_{max}	12.89	13.26	13.58	13.87	14.14	14.37	14.59
	n_{best}	12.14	12.51	12.83	13.13	13.39	13.63	13.86
	n_{min}	11.77	12.14	12.48	12.77	13.03	13.27	13.49
palaeo-DEM − 0.50 *m*	n_{max}	13.26	13.64	13.98	14.28	14.55	14.79	15.01
	n_{best}	12.46	12.85	13.18	13.48	13.77	14.02	14.25
	n_{min}	12.04	12.46	12.80	13.11	13.39	13.63	13.87
palaeo-DEM – 1.00 *m*	n_{max}	13.62	14.02	14.37	14.68	14.96	15.21	15.43
	n_{best}	12.75	13.17	13.52	13.84	14.13	14.40	14.64
	n_{min}	12.29	12.74	13.12	13.45	13.74	13.99	14.24
palaeo-DEM − 1.50 *m*	n_{max}	13.99	14.39	14.75	15.07	15.36	15.62	15.86
	n_{best}	13.02	13.48	13.85	14.19	14.48	14.77	15.02
	n_{min}	12.51	13.01	13.42	13.77	14.07	14.35	14.60
palaeo-DEM – 2.00 *m*	n_{max}	14.33	14.75	15.12	15.46	15.76	16.03	16.27
	n_{best}	13.27	13.76	14.17	14.52	14.83	15.12	15.39
	n_{min}	12.68	13.24	13.69	14.07	14.39	14.68	14.95
palaeo-DEM − 2.50 *m*	n_{max}	14.67	15.10	15.49	15.84	16.15	16.42	16.68
	n_{best}	13.48	14.03	14.47	14.84	15.17	15.46	15.75
	n_{min}	12.81	13.43	13.94	14.35	14.71	15.01	15.29
palaeo-DEM – 3.00 *m*	n_{max}	14.99	15.46	15.85	16.21	16.54	16.83	17.08
	n_{best}	13.67	14.28	14.76	15.16	15.50	15.82	16.10
	n_{min}	12.89	13.59	14.15	14.61	14.99	15.33	15.61
palaeo-DEM − 3.50 *m*	n_{max}	15.30	15.80	16.21	16.58	16.92	17.22	17.49
	n_{best}	13.81	14.48	15.02	15.45	15.82	16.14	16.43
	n_{min}	12.96	13.71	14.33	14.84	15.25	15.62	15.92

water level at Cologne and Düsseldorf-Urdenbach. Specifically, without considering the flows of the Sieg and Wupper tributaries, the maximum water levels at Cologne and Düsseldorf-Urdenbach corresponding to the discharge peaks from 12,000 m^3/s to 24,000 m^3/s at Remagen are lower from 0.11 m to 0.03 m at Cologne and from 0.13 m to 0.04 m at Düsseldorf-Urdenbach, respectively, compared to considering the flows of the Sieg and Wupper tributaries. This indicates that the larger the discharge peak at Remagen, the smaller the influence of the discharge of the Sieg and Wupper tributaries on the water levels at the Cologne and Düsseldorf-Urdenbach and vice versa.

4.5. Comparison with previous studies on the $Q_{max,1374}$

Reconstruction of the discharge magnitude of the 1374 flood event in the Rhine river has also been carried out in some previous studies (Herget and Meurs, 2010); Van Doornik, 2013). In the study of Herget and Meurs (2010), the peak discharge was estimated based on documentary data and a reconstruction of the river's cross-section, including estimations of channel incisions and anthropogenic modifications of the river and its floodplains. A simple cross-sectional approach was applied using Manning's equation (Eq. (2)) to take into account the roughness and channel geometry at Cologne only.

$$Q = AR^{2/3}S^{1/2}n^{-1} \quad (2)$$

where Q is discharge (m^3/s), A is wet cross-section area (m^2), R is hydraulic radius of flow (m), S is channel slope, n is the hydraulic roughness coefficient (s/$m^{/3}$).

Based on this approach, Herget and Meurs (2010) found a $Q_{max,1374}$ of around 23,200 m^3/s, with an uncertainty range of between 18,800 m^3/s and 29,000 m^3/s at Cologne considering maximum and minimum roughness coefficient. However, this uncertainty range was determined based only on the change in roughness coefficient without considering the uncertainty in the river bathymetry.

Van Doornik (2013) used a 2D hydraulic modelling approach to reconstruct the $Q_{max,1374}$. Based on this approach, Van Doornik (2013) found a peak discharge range of between 18,500 m3/s and 21,200 m3/s, and the most probable discharge was estimated to be 19,500 m3/s at Cologne. However, Van Doornik's study did not consider the uncertainty in the river bathymetry on the $Q_{max,1374}$ either due to the disadvantage of using 2D modelling related to computational costs. In addition, the $Q_{max,1374}$ values in Van Doornik's study were determined based on a water level (flood mark) of around 49.3 m asl without explanation for this selection, which is 1 m higher than the flood mark (48.28 m asl) at Cologne corresponding to the highest observed water level during the 1374 flood event. The flood mark elevation used in Van Doornik's study could be traced back to the wrong selection of the modern period reference level of the current gauge at Cologne in the conversion of the historic flood mark to the modern reference level. Instead of selecting the reference level of 34.98 m asl (the modern period reference level of the current gauge at Cologne), Van Doornik may have selected a

Table 4
The maximum water level at Düsseldorf-Urdenbach corresponding to the different combinations of river bed levels with Manning's n values and peak discharges – historic reconstructed maximum water level is 41.69 m asl. for Feb. 1374.

River bed level (m)	Manning roughness coefficient	Water level at Düsseldorf-Urdenbach (m)						
		12,000 (m^3/s)	14,000 (m^3/s)	16,000 (m^3/s)	18,000 (m^3/s)	20,000 (m^3/s)	22,000 (m^3/s)	24,000 (m^3/s)
palaeo-DEM	n_{max}	41.67	42.07	42.40	42.69	42.94	43.16	43.35
	n_{best}	40.89	41.31	41.68	42.01	42.29	42.54	42.76
	n_{min}	40.49	40.91	41.28	41.62	41.91	42.17	42.40
palaeo-DEM – 0.50 *m*	n_{max}	41.54	41.96	42.31	42.59	42.86	43.09	43.29
	n_{best}	40.72	41.15	41.53	41.86	42.17	42.43	42.67
	n_{min}	40.28	40.73	41.11	41.46	41.77	42.03	42.29
palaeo-DEM – 1.00 *m*	n_{max}	41.39	41.83	42.20	42.50	42.77	43.01	43.22
	n_{best}	40.53	40.97	41.37	41.72	42.03	42.31	42.56
	n_{min}	40.06	40.52	40.93	41.29	41.61	41.90	42.16
palaeo-DEM – 1.50 *m*	n_{max}	41.25	41.70	42.08	42.40	42.68	42.93	43.15
	n_{best}	40.32	40.79	41.20	41.57	41.89	42.19	42.45
	n_{min}	39.81	40.31	40.74	41.11	41.45	41.75	42.02
palaeo-DEM – 2.00 *m*	n_{max}	41.10	41.56	41.95	42.30	42.58	42.84	43.07
	n_{best}	40.09	40.60	41.03	41.40	41.74	42.05	42.32
	n_{min}	39.53	40.07	40.52	40.93	41.27	41.59	41.88
palaeo-DEM – 2.50 *m*	n_{max}	40.95	41.41	41.82	42.18	42.49	42.75	42.99
	n_{best}	39.84	40.39	40.84	41.23	41.58	41.90	42.19
	n_{min}	39.23	39.81	40.30	40.73	41.10	41.42	41.72
palaeo-DEM – 3.00 *m*	n_{max}	40.79	41.27	41.69	42.06	42.38	42.65	42.90
	n_{best}	39.58	40.16	40.64	41.05	41.41	41.74	42.05
	n_{min}	38.90	39.54	40.06	40.50	40.90	41.24	41.55
palaeo-DEM – 3.50 *m*	n_{max}	40.61	41.11	41.54	41.93	42.26	42.55	42.81
	n_{best}	39.30	39.91	40.43	40.86	41.24	41.58	41.89
	n_{min}	38.51	39.23	39.79	40.27	40.68	41.06	41.38

reference level of 35.98 m asl (1 m higher compared to the reference level of the current gauge at Cologne), which was used between 1782 and 1979. This is consistent with the difference in the elevation of flood marks used in these studies. Therefore, the $Q_{max,1374}$ in the study of Van Doornik (2013) might have been overestimated compared to the actual magnitude of this flood event.

Van der Meulen et al. (2021) performed hydraulic simulations of the pre-embankment situation to quantify the historic flood extents and magnitudes for the Late Holocene period in the Lower Rhine river valley and upper delta. Their simulations did not cover the flood events in late medieval times (1250–1500). Nevertheless, based on the comparison between simulated water levels and flood extents corresponding to each discharge value in the range of (10,000–30,000) m^3/s and the existing sedimentary records in the study area, they still suggested that only the lower end of the prediction of Herget and Meurs (2010) corresponding to a peak value of 18,800 m^3/s may be most realistic for the discharge magnitude of the 1374 flood event.

The results of this study and previous studies show a significant difference in the estimated $Q_{max,1374}$, and especially the results of Herget and Meurs (2010) differ significantly from other studies. The most apparent explanation is related to the differences in the input data used (e.g. river channel and floodplain geometry, hydraulic roughness coefficient, altitude of the gauge at Cologne) and approaches applied in these studies.

Regarding the accuracy of the input data, the topography and bathymetry of the river and floodplains are the most important inputs in hydraulic simulations to determine the discharge magnitude. In the present study, this information was extracted from a high-resolution palaeo-DEM for the early medieval time period of Van der Meulen et al. (2020). Although there is a significant difference in river bathymetry between Herget and Meurs's study and that used in the present study, this difference was here included through an uncertainty analysis. However, even in the case of a river bed level 3 m below the early medieval level extracted from the palaeo-DEM, which is the elevation of the river cross-section at Cologne that most closely resembles the elevation of the river cross-section used by Herget and Meurs (2010), the difference in the $Q_{max,1374}$ corresponding to best-guess Manning's *n* values in the two studies is still significant, 17,500 m^3/s compared to 23,200 m^3/s (approximately 33 %). This difference derives from the difference in the wet cross-section area of the river channel and floodplains at Cologne corresponding to the highest water level of 48.28 m asl during the 1374 flood event between the two studies. In the study of Herget and Meurs (2010), the wet cross-section area of the river channel and floodplains is 4900 m^2 and 10,900 m^2, respectively. In contrast, in this study, these values are 4200 m^2 and 9400 m^2. Thus, the wet cross-section area of the river channel and floodplain for the water level of 48.28 m asl corresponding to the best estimated $Q_{max,1374}$ in the study of Herget and Meurs (2010) is approximately 17 % and 16 % higher, respectively, compared to the wet cross-section area of the river channel and floodplain corresponding to the water level of 48.28 m asl in this

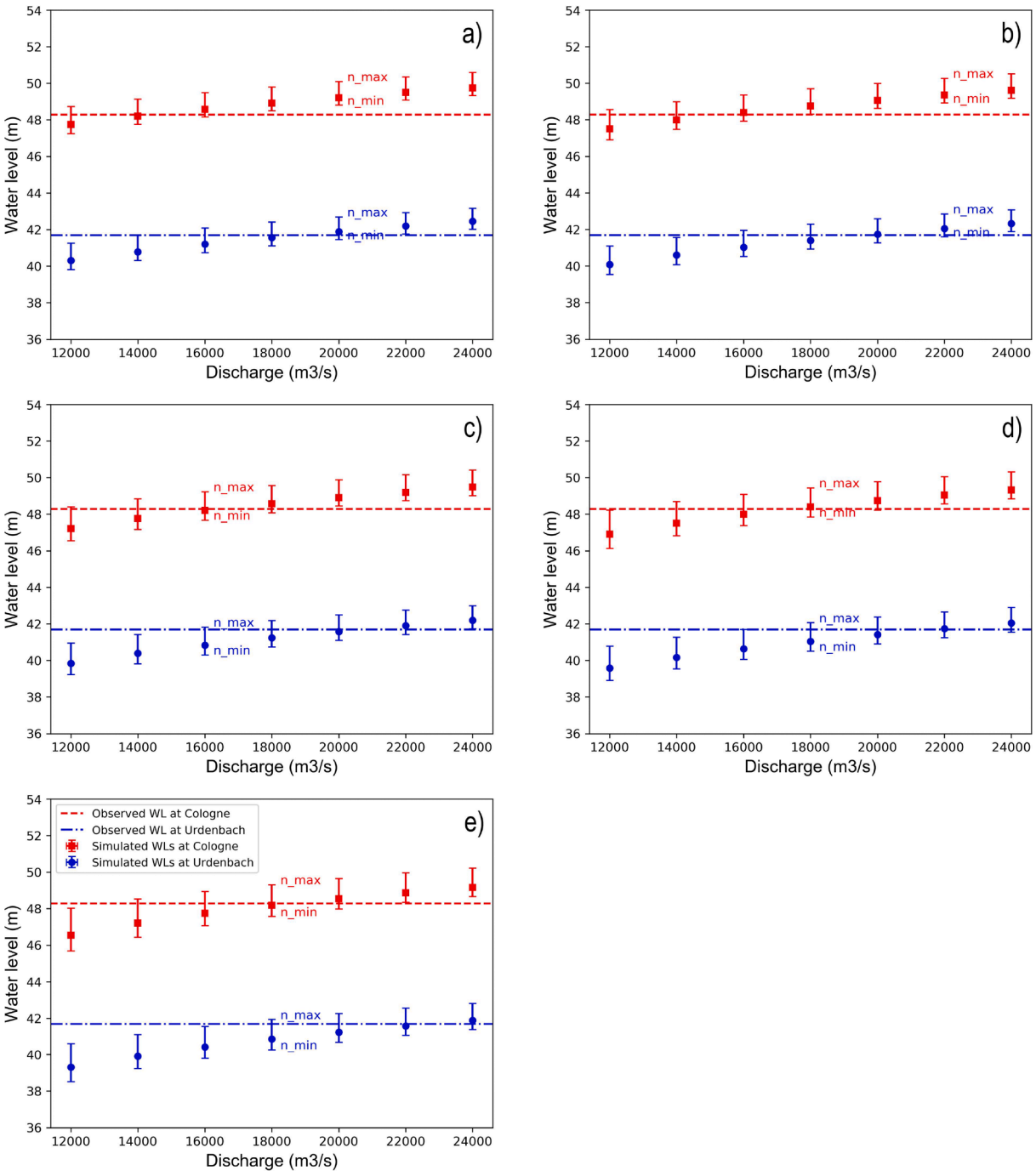

Fig. 10. Simulated water levels at Cologne and Düsseldorf-Urdenbach plotted against input peak discharges for river bed levels from 1.5 m to 3.0 m below the early medieval level extracted from the palaeo-DEM (Van der Meulen et al., 2020; Table 1), (a) – 1.5 m, (b) – 2.0 m, (c) – 2.5 m, (d) – 3.0 m, (e) – 3.5 m. The red and blue markers are the output water levels at Cologne and Düsseldorf-Urdenbach using best-guess Manning's *n* values and the uncertainty bands represent output for all roughness classes set to minimum and maximum Manning's *n* values (Van der Meulen et al., 2021a; Table 1).

study.

In addition to the wet area of cross-section, the difference in flow velocity in the river channel and floodplains at Cologne may also lead to the difference in the $Q_{max,1374}$ computed in the two studies. The difference in flow velocity derives from the difference in Manning's *n* values for landscape classes and applied approaches used in the two studies. The difference in Manning's *n* values for landscape classes between the two studies is shown in Table 6.

Manning's *n* values (n_{best}) for landscape classes in the study of Herget and Meurs (2010) in Table 6 are mean values for winter times used to determine the best-estimated $Q_{max,1374}$ (23,200 m^3/s). These values are lower than Manning's *n* values (n_{best}) for landscape classes used in this study. As a result, the flow velocity in Herget and Meurs's study is higher than the flow velocity in this study because the flow velocity is a function that depends on the inverse of the roughness coefficient (see Eq. (2)) (Chow, 1959).

Regarding applied approaches used in the two studies, Herget and Meurs (2010) used a simple cross-sectional approach, which can only calculate the variety of flow velocities in the different cross-section components like the river channel and floodplains for a cross-section at Cologne without considering the effect of other factors such as the river geometry, the distribution of the landscape classes, the effect of the

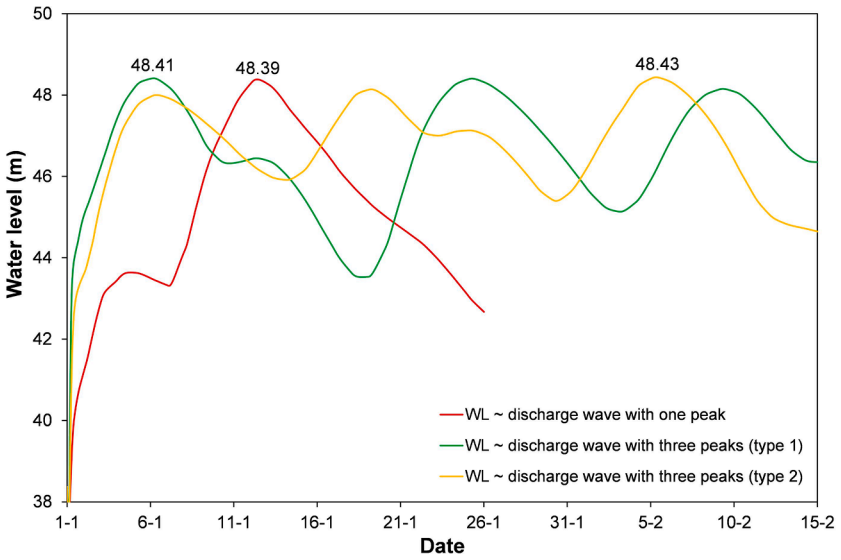

Fig. 11. Simulated water level time series at Cologne correspond to the inputs of three different discharge hydrograph shapes with the peak value of 18,000 m^3/s combined best-guess Manning's n value (n_{best}) and a river bed level 3 m below the early medieval level extracted from the palaeo-DEM.

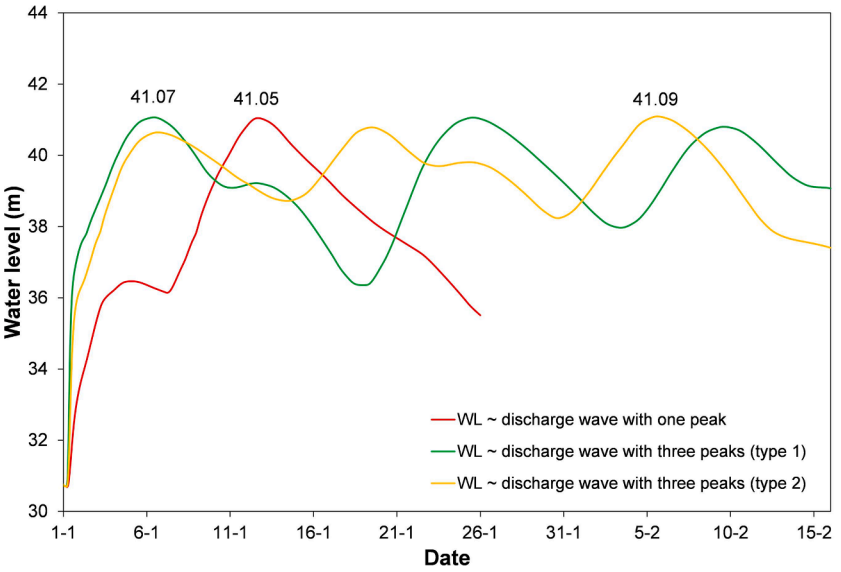

Fig. 12. Simulated water level time series at Düsseldorf-Urdenbach corresponding to the inputs of three different discharge hydrograph shapes with the peak value of 18,000 m^3/s combined best-guess Manning's n value (n_{best}) and a river bed level 3 m below the early medieval level extracted from the palaeo-DEM.

flows of tributaries, etc. around the interest location. In contrast, this study used the hydraulic modelling approach with 1D and 2D components, which can simulate the flow in the river channel and its floodplains to provide more accurate flow velocities and direction at all locations in the river system upstream and downstream of the cross-section for discharge estimation. This was demonstrated through using Manning's n values (n_{best}) in the study of Herget and Meurs (2010) for the case of a river bed level 3 m below the early medieval level extracted from the palaeo-DEM as mentioned above, the difference in the $Q_{max,1374}$ is still significant, 19,200 m^3/s (corresponding to flood mark level of 48.28 m at Cologne) compared to 23,200 m^3/s (approximately 21 %). While the difference in the river bathymetry and floodplain topography contributes approximately 16 % in the difference of the $Q_{max,1374}$ as discussed above. Therefore, the remaining difference comes from the approaches used in the two studies. In other words, the applied approaches also contribute to the difference in the $Q_{max,1374}$ between the two studies Table 7.

4.6. The magnitude of design discharges

Flood frequency analysis based on the discharge data extended with the $Q_{max,1374}$ of this study results in a design discharge with a 100,000 year return period (the value used as maximum safety standard in the Dutch water policy) and 95 % confidence interval of 15,700 m^3/s and 4,200 m^3/s (Fig. 16), respectively. In comparison, these numbers are 17,700 m^3/s and 4,900 m^3/s (Fig. 13) when using the $Q_{max,1374}$ computed by Herget and Meurs (2010). Hence, updating the $Q_{max,1374}$ of this study into the flood frequency analysis results in a significant reduction of 2,000 m^3/s (11.8 %) in the design discharge and 700 m^3/s (14.3 %) in the confidence interval corresponding to a 100,000 year return period compared to using the 1374 reconstructed discharge magnitude of Herget and Meurs (2010). This reduction in the design discharge magnitude may significantly reduce the investment cost of protection measures along the Rhine river. The reduction of the 95 % confidence interval shows the importance of reconstructing historic

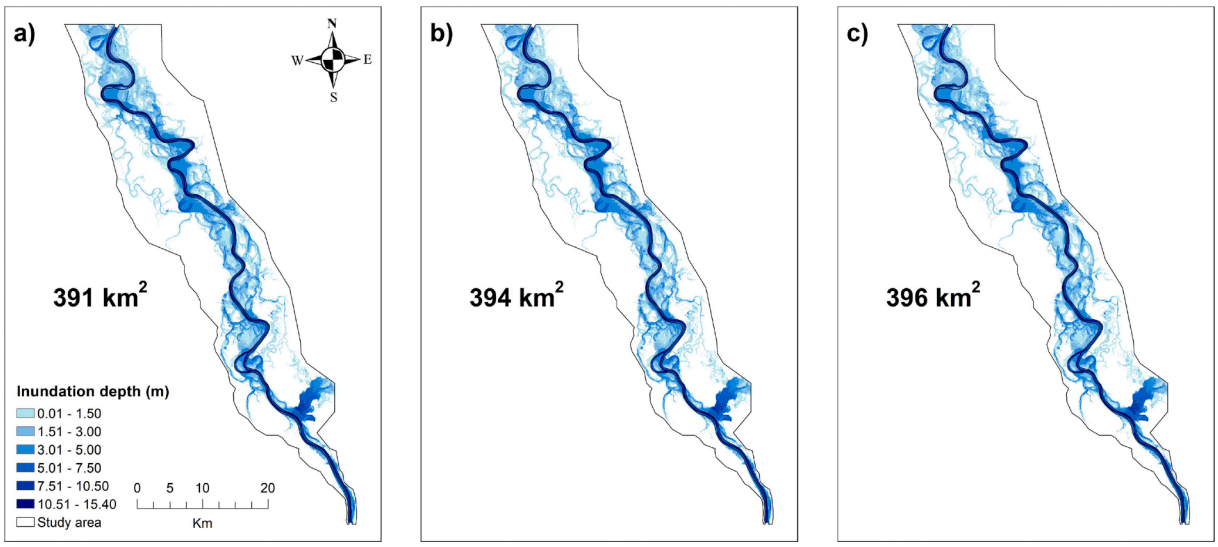

Fig. 13. Inundation maps corresponding to the inputs of three different flood hydrograph shapes (a) one peak, (b) three peaks type 1, (c) three peaks type 2) with the peak value of 18,000 m^3/s combined best-guess Manning's n value (n_{best}) and a river bed level 3 m below the early medieval level extracted from the palaeo-DEM.

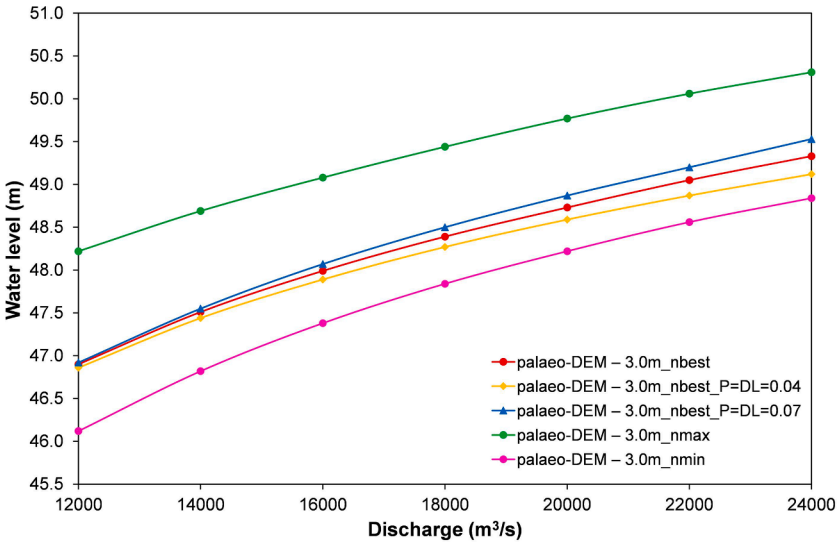

Fig. 14. Simulated maximum water levels at Cologne corresponding to the inputs of peak discharges with different Manning's n values (n_{max}, n_{best}, and n_{min}) for a river bed level 3 m below the early medieval level extracted from the palaeo-DEM. Pink, red, and green curves show water levels corresponding to the reconstructed distribution of five landscape classes of Van der Meulen et al. (2021a) for minimum, best-guess and maximum Manning's n values respectively. Meanwhile, yellow and blue curves show water levels corresponding to the adjusted distribution of landscape by merging P zone with DL zone, with assigned roughness values of 0.04 and 0.07 ($s/m^{/3}$), respectively.

flood events with high accuracy since design discharges can now be predicted with more certainty.

4.7. A comparison with Bayesian Markov chain Monte Carlo statistical methods

The use of different methods in flood frequency analysis result in the difference in design discharges. The present study inherited the approach of Bomers et al. (2019a) to include historic flood information in flood safety assessments. With this approach, the length of the measured discharge data set is extended using the bootstrap method while the general approach of the flood frequency analysis is still kept. In addition, the bootstrap method is not only used to extend the data set for the missing years, but also to sample annual maximum discharges based on the uncertainty ranges of reconstructed historic flood events. This reduces the uncertainty in design discharges corresponding to large return periods.

In addition to the approach applied in this study, Bayesian Markov chain Monte Carlo (MCMC) statistical methods can also account for historical information including their uncertainties in flood frequency analysis (Gaume, 2018; Payrastre et al., 2011; Reis and Stedinger, 2005). However, Bayesian methods also have several limitations, in which selecting a statistical distribution (a theoretical mathematical function) for the numerical derivations is required to be fitted to the data sets. It means that the results depend on a priori parameters (Gaume, 2018). Therefore, the posterior distributions are highly influenced by the prior distributions, which may result in a larger uncertainty of flood frequency relations compared to the influence caused by the errors in discharge measurements (Neppel et al., 2010). The maximum likelihood method can be used to estimate the prior distribution based on the measured data. However, in this case, there were no discharge measurements near the tail of the distributions. Therefore, the advantages of the Bayesian MCMC method compared to a traditional flood frequency analysis method still need to be investigated. In addition, further studies on the difference in uncertainty estimates between the proposed bootstrap method in Bomers et al. (2019a) and Bayesian MCMC methods are needed.

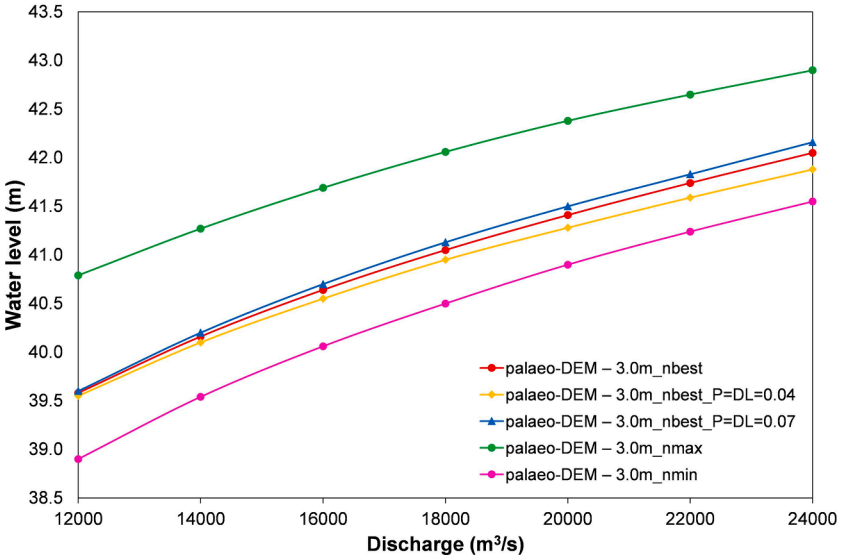

Fig. 15. Simulated maximum water levels at Düsseldorf-Urdenbach corresponding to the inputs of peak discharges with different Manning's n values (n_{max}, n_{best}, and n_{min}) for a river bed level 3 m below the early medieval level extracted from the palaeo-DEM. Pink, red, and green curves show water levels corresponding to the reconstructed distribution of five landscape classes of Van der Meulen et al. (2021a) for minimum, best-guess and maximum Manning's n values respectively. Meanwhile, yellow and blue curves show water levels corresponding to the adjusted distribution of landscape by merging P zone with DL zone, with assigned roughness values of 0.04 and 0.07 ($s/m^{1/3}$), respectively.

Table 5
The maximum water levels at Cologne and Düsseldorf-Urdenbach corresponding to the simulations that include and exclude the inflows of the Sieg and Wupper tributaries for combinations of Manning's n values (nbest) and river bed level 3 m below the early medieval level extracted from the palaeo-DEM.

Discharge (m^3/s)	12,000 (m^3/s)	14,000 (m^3/s)	16,000 (m^3/s)	18,000 (m^3/s)	20,000 (m^3/s)	22,000 (m^3/s)	24,000 (m^3/s)
Water level at Cologne (m)							
With the Sieg and Wupper tributaries	46.90	47.51	47.99	48.39	48.73	49.05	49.33
Without the Sieg and Wupper tributaries	46.79	47.43	47.92	48.33	48.68	49.01	49.30
Water level at Düsseldorf-Urdenbach (m)							
With the Sieg and Wupper tributaries	39.58	40.16	40.64	41.05	41.41	41.74	42.05
Without the Sieg and Wupper tributaries	39.45	40.05	40.55	40.97	41.35	41,69	42.01

Table 6
Comparison of hydraulic roughness coefficient corresponding to landscape classes between the present study and Herget and Meurs (2010)'s study.

Manning's n value		n_{min} ($s/m^{1/3}$)		n_{best} ($s/m^{1/3}$)		n_{max} ($s/m^{1/3}$)	
Classification (source; Van der Meulen et al. (2021a))		This study	Herget and Meurs (2010)	This study	Herget and Meurs (2010)	This study	Herget and Meurs (2010)
H	High grounds	0.1	x	0.1	x	0.1	x
R	River bed and banks	0.025	0.024	0.03	0.027	0.045	0.030
P	Proximal floodplain *	0.06	0.033	0.07	0.044	0.08	0.058
DH	Distal floodplain, high *	0.04	0.033	0.05	0.044	0.06	0.058
DL	Distal floodplain, low **	0.035	0.029	0.04	0.036	0.055	0.047

Manning's n values used in the study of Herget and Meurs (2010) in Table 6 are values for winter conditions.
* floodplain class inHerget and Meurs (2010).
** floodplain channels class inHerget and Meurs (2010).
x: outside cross-section in Herget and Meurs (2010).

4.8. The advantages of using a 1D-2D coupled hydraulic modelling approach in reconstructing historic flood events

This study shows that using a 1D-2D coupled hydraulic modelling approach allows performing an uncertainty analysis to investigate the effect of inherent uncertain parameters (e.g. river bathymetry, hydraulic roughness) on the discharge magnitude of historic flood events with acceptable computational cost (approximate 40 min for each simulation). Schematizing the main river by 1D profiles allows the adjustment of the river bed level (river bathymetry) in a flexible way to facilitate an uncertainty analysis, which can also be resolved by a 2D modelling approach through indirect adjustment of DEM data for a 2D model. However, such a 2D adjustment is more time-consuming. In addition, simulating floodplains by 2D grids takes the complex flow structures in the river floodplains much better into account compared to a simple approach (Baker, 2008; Benito and Díez-Herrero, 2014; Herget and Meurs, 2010; Webb and Jarrett, 2002), even though the 2D approach requires more detailed input data (e.g. the topography of floodplains, land use classes) compared to the simple cross-sectional approach of Herget and Meurs (2010).

Furthermore, using the 1D-2D coupled hydraulic modelling approach allows the investigation of the effect of discharge magnitude and flood hydrograph shape on flow parameters (flow velocity, flow depth). In contrast, a simple approach can only consider the effect of the discharge magnitude on flow parameters (Herget and Meurs, 2010; Herget et al., 2014).

5. Conclusions

In this study, a 1D-2D coupled hydraulic modelling approach was used to reconstruct the 1374 historic peak discharge ($Q_{max,1374}$) in the Rhine river. We found that this modelling approach has benefits for historic flood reconstructions compared to previous approaches (e.g. 1D cross-sectional approach, fully 2D hydraulic modelling approach). The 1D-2D modelling approach allows adjusting river bathymetry data more flexible and much faster compared to the 2D modelling approach in

Table 7
The maximum water level at Cologne corresponding to the different combinations of river bed level 3 m below the early medieval level extracted from the palaeo-DEM with Manning's n values (n_{best}) used in Herget and Meurs (2010)'s study and peak discharges.

Discharge (m^3/s)	12,000 (m^3/s)	14,000 (m^3/s)	16,000 (m^3/s)	18,000 (m^3/s)	20,000 (m^3/s)	22,000 (m^3/s)	24,000 (m^3/s)
Water level (m)	46.44	47.09	47.61	48.06	48.42	48.71	48.98

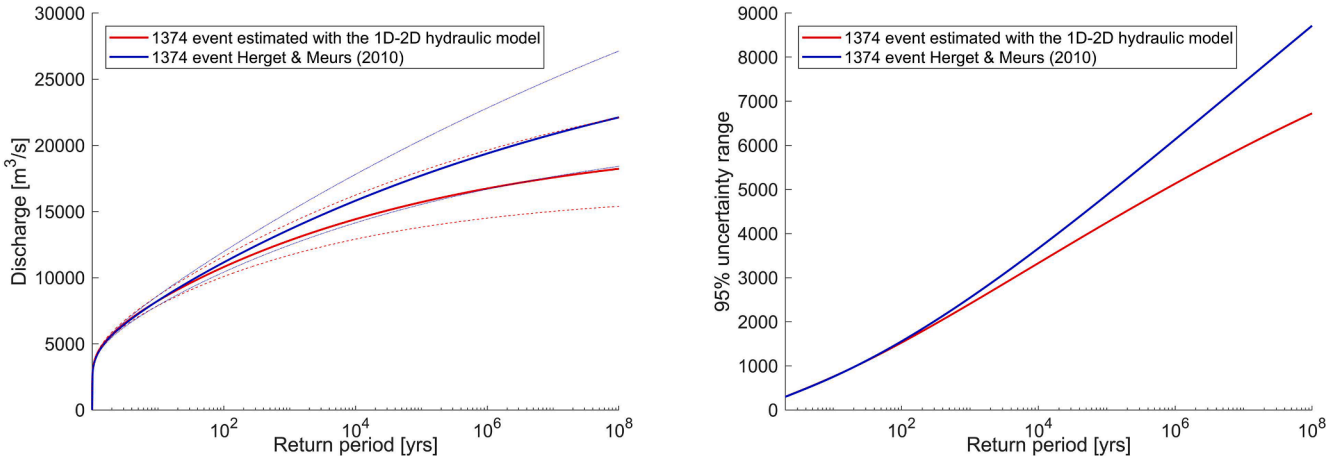

Fig. 16. Flood frequency curves and their 95 % confidence intervals of data sets when using the $Q_{max,1374}$ corresponding to Herget and Meurśs study and this study.

performing an uncertainty analysis to investigate the effect of the inherent uncertainties in reconstructing the historic terrain (river bathymetry and floodplains topography) and hydraulic roughness of the historic landscape on the discharge magnitude of historic flood events.

The study's results show that the value of the peak discharge during the 1374 flood event, $Q_{max,1374}$, is between 14,400 m^3/s and 18,500 m^3/s near Remagen, Germany. Furthermore, this study showed that the effect of potential flood hydrograph shapes, the spatial distribution of the Proximal floodplain land cover class in the land cover map in the Rhine river, and the flows of the Sieg and Wupper tributaries does not have a significant impact on the highest (peak) water levels along the river in the study area in the pre-embankment era. A flood frequency analysis of annual maximum peak flow data including the 1374 historic flood event derived in this study, results in the design discharge corresponding to the 100,000 year return period in the Rhine river of 15,700 m^3/s, which is 2,000 m^3/s lower than the $Q_{max,1374}$ estimation of Herget and Meurs (2010).

Declaration of Competing Interest

The authors declare that they have no known competing financial interests or personal relationships that could have appeared to influence the work reported in this paper.

Data availability

Data will be made available on request.

Acknowledgements

This research has been supported by the NWO (project no. 14506), which is partly funded by the Ministry of Economic Affairs and Climate Policy.

The authors would like to thank Dr. Daniel Schwand (Bundesanstalt für Gewässerkunde) for providing unpublished discharge data of River Wupper and Wolfgang Keil for providing background information on the water-level marker at Urdenbach.

References

Adeogun, A.G., Daramola, M.O., Pathirana, A., 2015. Coupled 1D–2D hydrodynamic inundation model for sewer overflow: Influence of modeling parameters. Water Sci. 29, 146–155. https://doi.org/10.1016/j.wsj.2015.12.001.

Alexandre, P., 1987. Le climat en Europe au Moyen Age, contribution à l'histoire des variations climatiques de 1000 à 1425, d'après les sources narratives de l'Europe occidentale. Editions de l'Ecole des hautes études en sciences sociales, Paris.

Alfieri, L., Burek, P., Feyen, L., Forzieri, G., 2015. Global warming increases the frequency of river floods in Europe. Hydrol. Earth Syst. Sci. 19, 2247–2260. https://doi.org/10.5194/hess-19-2247-2015.

Alfieri, L., Bisselink, B., Dottori, F., Naumann, G., Wyser, K., Feyen, L., De Roo, A., 2017. Earth's Future Global projections of river flood risk in a warmer world Earth's Future. https://doi.org/10.1002/eft2.183.

Arnell, N.W., Gosling, S.N., 2016. The impacts of climate change on river flood risk at the global scale 387–401. https://doi.org/10.1007/s10584-014-1084-5.

Baker, V.R., 2008. Paleoflood hydrology: Origin, progress, prospects. Geomorphology 101, 1–13. https://doi.org/10.1016/j.geomorph.2008.05.016.

Balasch, J.C., Ruiz-Bellet, J.L., Tuset, J., Martin De Oliva, J., 2010. Reconstruction of the 1874 Santa Tecla's rainstorm in Western Catalonia (NE Spain) from flood marks and historical accounts. Nat. Hazards Earth Syst. Sci. 10, 2317–2325. https://doi.org/10.5194/nhess-10-2317-2010.

Baynes, E.R.C., Attal, M., Niedermann, S., Kirstein, L.A., Dugmore, A.J., Naylor, M., 2015. Erosion during extreme flood events dominates holocene canyon evolution in northeast iceland. Proc. Natl. Acad. Sci. U. S. A. 112, 2355–2360. https://doi.org/10.1073/pnas.1415443112.

Benito, G., Díez-Herrero, A., 2014. Palaeoflood Hydrology: Reconstructing rare events and extreme flood discharges. In Schroder, J., Paron, P., Di Baldassarre, G. (Eds.) Hydro-Meteorological Hazards, Risks, and Disasters. https://doi.org/10.1016/B978-0-12-394846-5.00003-5.

Benito, G., Thorndycraft, V.R., 2004. Systematic, Palaeoflood and Historical Data for the Improvement of Flood Risk Estimation: Methodological Guidelines. CSIC, Madrid, p. 115.

Benito, G., Castillo, O., Ballesteros-Cánovas, J.A., MacHado, M., Barriendos, M., 2021. Enhanced flood hazard assessment beyond decadal climate cycles based on centennial historical data (Duero basin, Spain). Hydrol. Earth Syst. Sci. 25, 6107–6132. https://doi.org/10.5194/hess-25-6107-2021.

Bezak, N., Brilly, M., Šraj, M., 2014. Comparison between the peaks-over-threshold method and the annual maximum method for flood frequency analysis. Hydrol. Sci. J. 59, 959–977. https://doi.org/10.1080/02626667.2013.831174.

Bomers, A., Schielen, R.M.J., Hulscher, S.J.M.H., 2019a. Decreasing uncertainty in flood frequency analyses by including historic flood events in an efficient bootstrap approach. Nat. Hazards Earth Syst. Sci. 19, 1895–1908. https://doi.org/10.5194/nhess-19-1895-2019.

Bomers, A., Van der Meulen, B., Schielen, R.M.J., Hulscher, S.J.M.H., 2019b. Historic Flood Reconstruction With the Use of an Artificial Neural Network. Water Resour. Res. 55, 9673–9688. https://doi.org/10.1029/2019WR025656.

Bomers, A., Schielen, R.M.J., Hulscher, S.J.M.H., 2019c. Application of a lower-fidelity surrogate hydraulic model for historic flood reconstruction. Environ. Model. Softw. 117, 223–236. https://doi.org/10.1016/j.envsoft.2019.03.019.

Bomers, A., Schielen, R.M.J., Hulscher, S.J.M.H., 2019d. The Severe 1374 Rhine River Flood Event in Present Times. 38th IAHR World Congr. - "Water Connect. World" 38, 1764–1773. https://doi.org/10.3850/38wc092019-0501.

Brázdil, R., Demarée, G.R., Deutsch, M., Garnier, E., Kiss, A., Luterbacher, J., Macdonald, N., Rohr, C., Dobrovolný, P., Kolář, P., Chromá, K., 2010. European floods during the winter 1783/1784: Scenarios of an extreme event during the "Little Ice Age". Theor. Appl. Climatol. 100, 163–189. https://doi.org/10.1007/s00704-009-0170-5.

Brunner, G.W., 2016. HEC-RAS, River Analysis System – 2D Modelling User's Manual, Version 5.0. US Army Corps of Engineers Hydrologic Engineering Center (HEC), Davis, USA. 1–962.

Buismann, J., 1996. Duizend Jaar Weer, Wind en Water in de lage Lande. Deel 2, 1300-1450. Uitgeverij Van Wijnen, Franeker.

Cameron, D.S., Beven, K.J., Tawn, J., Blazkova, S., Naden, P., 1999. Flood frequency estimation by continuous simulation for a gauged upland catchment (with uncertainty). J. Hydrol. 219, 169–187. https://doi.org/10.1016/S0022-1694(99)00057-8.

Cardoso, M.A., Almeida, M.C., Brito, R.S., Gomes, J.L., Beceiro, P., Oliveira, A., 2020. 1D/2D stormwater modelling to support urban flood risk management in estuarine areas: Hazard assessment in the Dafundo case study. J. Flood Risk Manag. 13, 1–15. https://doi.org/10.1111/jfr3.12663.

Chow, V.T., 1959. Open channel hydraulics. McGraw-Hill, New York.

Costabile, P., Macchione, F., Natale, L., Petaccia, G., 2015. Comparison of scenarios with and without bridges and analysis of backwater effect in 1-D and 2-D river flood modeling. C. - Comput. Model. Eng. Sci. 109, 81–103. https://doi.org/10.3970/cmes.2015.109.081.

Dasallas, L., Yeonsu, K., Hyunuk, A., 2019. Case study of HEC-RAS 1D–2D coupling simulation: 2002 Baeksan flood event in Korea. Water (Switzerland) 11, 1–14. https://doi.org/10.3390/w11102048.

Dung, N.V., Merz, B., Bárdossy, A., Apel, H., 2015. Handling uncertainty in bivariate quantile estimation - An application to flood hazard analysis in the Mekong Delta. J. Hydrol. 527, 704–717. https://doi.org/10.1016/j.jhydrol.2015.05.033.

Elleder, L., Herget, J., Roggenkamp, T., Nießen, A., 2013. Historic floods in the city of Prague - A reconstruction of peak discharges for 1481–1825 based on documentary sources. Hydrol. Res. 44, 202–214. https://doi.org/10.2166/nh.2012.161.

Engeland, K., Wilson, D., Borsányi, P., Roald, L., Holmqvist, E., 2018. Use of historical data in flood frequency analysis: A case study for four catchments in Norway. Hydrol. Res. 49, 466–486. https://doi.org/10.2166/nh.2017.069.

Erkens, G., Hoffmann, T., Gerlach, R., Klostermann, J., 2011. Complex fluvial response to Lateglacial and Holocene allogenic forcing in the Lower Rhine Valley (Germany). Quat. Sci. Rev. 30, 611–627. https://doi.org/10.1016/j.quascirev.2010.11.019.

Fan, Y., Ao, T., Yu, H., Huang, G., Li, X., 2017. A coupled 1D–2D hydrodynamic model for urban flood inundation. Adv. Meteorol. 2017 https://doi.org/10.1155/2017/2819308.

Frances, F., Salas, J.D., Boes, D.C., 1994. Flood frequency analysis with systematic and historical or paleoflood data based on the two-parameter general extreme value models. Water Resour. Res. 30 (6), 1653–1664. https://doi.org/10.1029/94WR00154.

Gaume, E., 2018. Flood frequency analysis: The Bayesian choice. Wiley Interdiscip. Rev. Water 5, 1–11. https://doi.org/10.1002/WAT2.1290.

Gebregiorgis, A.S., Hossain, F., 2012. Hydrological Risk Assessment of Old Dams: Case Study on Wilson Dam of Tennessee River Basin. J. Hydrol. Eng. 17, 201–212. https://doi.org/10.1061/(asce)he.1943-5584.0000410.

Hansen, J., 1899. Arnold Mercator und die wiederentdeckten Kölner Stadtpläne von 1571 und 1642. Mitteilungen aus dem Stadtarchiv Köln, p. 28.

Hegnauer, M., Beersma, J., Van den Boogaard, H., Buishand, T., Passchier, R. 2014. Generator of Rainfall and Discharge Extremes (GRADE) for the Rhine and Meuse basins. Final Report of GRADE 2.0. Technical Report, Deltares, Delft, The Netherlands.

Hegnauer, M., Kwadijk, J., Klijn, F., 2015. The plausibility of extreme high discharges in the river Rhine. Tech, Rep.

Herget, J., Meurs, H., 2010. Reconstructing peak discharges for historic flood levels in the city of Cologne. Germany. Glob. Planet. Change 70, 108–116. https://doi.org/10.1016/j.gloplacha.2009.11.011.

Hirabayashi, Y., Mahendran, R., Koirala, S., Konoshima, L., Yamazaki, D., Watanabe, S., Kim, H., Kanae, S., 2013. Global flood risk under climate change. Nat. Clim. Chang. 3, 4–6. https://doi.org/10.1038/nclimate1911.

ENW Hoogwater, 2021. Hoogwater 2021: Feiten en Duiding, 158.

Horritt, M.S., Bates, P.D., 2002. Evaluation of 1D and 2D numerical models for predicting river flood inundation. J. Hydrol. 268 (1–4), 87–99. https://doi.org/10.1016/S0022-1694(02)00121-X.

Jasmund, R., 1901. Die Arbeiten der Rheinstrom-Bauverwaltung 1851–1900. Buchdruck des Waisenhauses, Halle.

Klostermann, J., 1992. Das Quartär der Niederrheinischen Bucht. Geologisches Landesamt Nordrhein-Westfalen, Krefeld, p. 200.

Krahe, P., 1997. Hochwasser und Klimafluktuation am Rhein seit dem Mittelalter. Immendorf (Eds) Hochwasser - Natur im Überfluß? Müller Heidelberg 57–82.

Lang, M., Moussay, D., Recking, A., Naulet, R., 2003. Hydraulic modelling of historical floods: a case study on the Ardeche river at Vallon-Pont-D'arc. In Thorndycraft VR, Benito G, Barriendos M, Llasat C (eds.) Palaeofloods, Historical Data & Climatic Variability: Applications in Flood Risk Assessment (Proceedings of the PHEFRA International Workshop, Barcelona, 16-19th. October 2002) CSIC Madrid. 183-189.

Lang, M., Fernández Bono, J.F., Recking, A., Naulet, R., Grau Gimeno, P., 2004. Methodological guide for palaeoflood and historical peak discharge estimation, in Palaeofloods, Historical Data and Climatic Variability: Applications in Flood Risk Assessment, edited by Benito, G., Thorndycraft, V.R., pp. 43–53, CSIC, Madrid, 115pp.

Lang, M., Ouarda, T.B.M.J., Bobée, B., 1999. Towards operational guidelines for over-threshold modeling. J. Hydrol. 225 (3–4), 103–117. https://doi.org/10.1016/S0022-1694(99)00167-5.

Leandro, J., Martins, R., 2016. A methodology for linking 2D overland flow models with the sewer network model SWMM 5.1 based on dynamic link libraries. Water Sci. Technol 73, 3017–3026. https://doi.org/10.2166/wst.2016.171.

MacDonald, N., Kjeldsen, T.R., Prosdocimi, I., Sangster, H., 2014. Reassessing flood frequency for the Sussex Ouse, Lewes: The inclusion of historical flood information since AD 1650. Nat. Hazards Earth Syst. Sci. 14, 2817–2828. https://doi.org/10.5194/nhess-14-2817-2014.

Matsumoto, D., Sawai, Y., Yamada, M., Namegaya, Y., Shinozaki, T., Takeda, D., Fujino, S., Tanigawa, K., Nakamura, A., Pilarczyk, J.E., 2016. Erosion and sedimentation during the September 2015 flooding of the Kinu River, central Japan. Sci. Rep. 6, 1–10. https://doi.org/10.1038/srep34168.

Neppel, L., Renard, B., Lang, M., Ayral, P.A., Coeur, D., Gaume, E., Jacob, N., Payrastre, O., Pobanz, K., Vinet, F., 2010. Flood frequency analysis using historical data: Accounting for random and systematic errors. Hydrol. Sci. J. 55, 192–208. https://doi.org/10.1080/02626660903546092.

O'Connell, D.R.H., Ostenaa, D.A., Levish, D.R., Klinger, R.E., 2002. Bayesian flood frequency analysis with paleohydrologic bound data, 16–1-16–13 Water Resour. Res. 38. https://doi.org/10.1029/2000wr000028.

Pasquier, U., He, Y., Hooton, S., Goulden, M., Hiscock, K.M., 2019. An integrated 1D–2D hydraulic modelling approach to assess the sensitivity of a coastal region to compound flooding hazard under climate change. Nat. Hazards 98, 915–937. https://doi.org/10.1007/s11069-018-3462-1.

Payrastre, O., Gaume, E., Andrieu, H., 2011. Usefulness of historical information for flood frequency analyses: Developments based on a case study. Water Resour. Res. 47, 1–15. https://doi.org/10.1029/2010WR009812.

Pol, J., 2014. Hydrograph shape variability on the river Meuse – Evaluation of design hydrograph methods and probabilistic methods to estimate design water levels on the river Meuse. Master thesis, Dept. of Hydraulic Engineering, Delft University of Technology, the Netherlands.

Reis, D.S., Stedinger, J.R., 2005. Bayesian MCMC flood frequency analysis with historical information. J. Hydrol. 313, 97–116. https://doi.org/10.1016/j.jhydrol.2005.02.028.

Ruiz-Bellet, J.L., Balasch, J.C., Tuset, J., Barriendos, M., Mazón, J., 2014. Spatial extension of the reconstruction of 1874 Santa Tecla's flash floods in Catalonia (NE Iberian Peninsula) 16, 8076.

Sartor, J., Zimmer, K.H., Busch, N., 2010. Historische Hochwasserereignisse der deutschen Mosel. Wasser und Abfall 12, 46–51. https://doi.org/10.1007/bf03247674.

Schendel, T., Thongwichian, R., 2017. Considering historical flood events in flood frequency analysis: Is it worth the effort? Adv. Water Resour. 105, 144–153. https://doi.org/10.1016/j.advwatres.2017.05.002.

Stamataki, I., Kjeldsen, T.R., 2021. Reconstructing the peak flow of historical flood events using a hydraulic model: The city of Bath. United Kingdom. J. Flood Risk Manag. 14, 1–15. https://doi.org/10.1111/jfr3.12719.

Stanley, J.D., Goddio, F., Schnepp, G., 2001. Nile flooding sank two ancient cities. Nature 412, 293–294. https://doi.org/10.1038/35085628.

Te Linde, A.H., Bubeck, P., Dekkers, J.E.C., De Moel, H., Aerts, J.C.J.H., 2011. Future flood risk estimates along the river Rhine. Nat. Hazards Earth Syst. Sci. 11, 459–473. https://doi.org/10.5194/nhess-11-459-2011.

Teraguchi, H., Nakagawa, H., Kawaike, K., Baba, Y., Zhang, H., 2011. Effects of hydraulic structures on river morphological processes. Int. J. Sediment Res 26 (3), 283–303. https://doi.org/10.1016/S1001-6279(11)60094-2.

Toonen, W.H.J., De Molenaar, M.M., Bunnik, F.P.M., Middelkoop, H., 2013. Middle Holocene palaeoflood extremes of the Lower Rhine. Hydrol. Res. 44, 248–263. https://doi.org/10.2166/nh.2012.162.

Toonen, W.H.J., Winkels, T.G., Cohen, K.M., Prins, M.A., Middelkoop, H., 2015. Lower Rhine historical flood magnitudes of the last 450years reproduced from grain-size measurements of flood deposits using End Member Modelling. Catena 130, 69–81. https://doi.org/10.1016/j.catena.2014.12.004.

Toonen, W.H.J., 2013. A Holocene flood record of the Lower Rhine, Utrecht Studies in Earth Sciences.

Van Alphen, J., 2016. The Delta Programme and updated flood risk management policies in the Netherlands. J. Flood Risk Manag. 9 (4), 310–319. https://doi.org/10.1111/jfr3.12183.

Van der Meulen, B., Cohen, K.M., Pierik, H.J., Zinsmeister, J.J., Middelkoop, H., 2020. LiDAR-derived high-resolution palaeo-DEM construction workflow and application to the early medieval Lower Rhine valley and upper delta. Geomorphology 370, 107370. https://doi.org/10.1016/j.geomorph.2020.107370.

Van der Meulen, B., Bomers, A., Cohen, K.M., Middelkoop, H., 2021. Late Holocene flood magnitudes in the Lower Rhine river valley and upper delta resolved by a two-dimensional hydraulic modelling approach. Earth Surf. Process. Landforms 46, 853–868. https://doi.org/10.1002/esp.5071.

Van der Meulen, B., Defilet, M.P., Tebbens, L.A., Cohen, K.M., 2022. Palaeoflood level reconstructions in a lowland setting from urban archaeological stratigraphy, Rhine river delta, the Netherlands. Catena 212, 106031. https://doi.org/10.1016/j.catena.2022.106031.

Van der Meulen, B., 2021b. River flood reconstruction in the Lower Rhine valley and delta. PhD thesis, Faculty of Geosciences, Utrecht University, the Netherlands.

Van Doornik, W.E., 2013. Reconstructie van het hoogwater in de Rijn van 1374 en de gevolgen voor de huidige situatie 18.000 m^3/s: waan of werkelijkheid. Master thesis, Dept. of Water Engineering & Management, University of Twente, the Netherlands.

Van, T.P.D., Popescu, I., Griensven, A.V., Brussel, V.U., 2012. A study of the climate change impacts on fluvial flood propagation in the Vietnamese Mekong Delta. Hydrol. Earth Syst. Sci. Discuss. 9, 7227–7270. https://doi.org/10.5194/hessd-9-7227-2012.

Vorogushyn, S., Lindenschmidt, K.E., Kreibich, H., Apel, H., Merz, B., 2012. Analysis of a detention basin impact on dike failure probabilities and flood risk for a channel-dike-floodplain system along the river Elbe. Germany. J Hydrol. 436, 120–131. https://doi.org/10.1016/j.jhydrol.2012.03.006.

Webb, R.H., Jarrett, R.D., 2002. One-dimensional estimation techniques for discharges of paleofloods and historical floods. In: House PK, Webb RH, Baker VR, Levish DR (Eds.) Ancient Floods, Modern Hazards: Principles and Applications of Paleoflood Hydrology. Water Science and Application, Vol. 5, pp. 111–125.

Weikinn, C., 1958. Quellentexte zur Witterungsgeschichte Europas von der Zeitenwende bis zum Jahr 1850 – Band 1. Akademie-Verlag, Berlin.

Wu, L., Zhu, C., Zheng, C., Li, F., Wang, X., Li, L., Sun, W., 2014. Holocene environmental change and its impacts on human settlement in the shanghai area, East China. Catena 114, 78–89. https://doi.org/10.1016/j.catena.2013.10.012.

Zhang, Q., Zhu, C., Liu, C.L., Jiang, T., 2005. Environmental change and its impacts on human settlement in the Yangtze Delta, P.R. China. Catena 60, 267–277. https://doi.org/10.1016/j.catena.2004.12.001.